Reviewed Preprint
v1 • May 22, 2026
Not revised

For correspondence: kkroll@wustl.edu

# Equal contribution

Competing interests: No competing interests declared

Funding: See page 19

Reviewing editor: Anne E West, Duke University, United States

Tatton-Brown-Rahman Syndrome-associated *DNMT3A* mutations de-repress cortical interneuron differentiation to disrupt neuronal network function

Gareth Chapman[1,#], Julianna J Determan[1,#], John R Edwards[2], Faiza Batool[1], James E Huettner[3], Ramachandran Prakasam[1], Sydney R Crump[1], Travis E Law[2,4], Haley Jetter[1], Harrison W Gabel[4], Kristen L Kroll[1]

[1]Department of Developmental Biology, Washington University School of Medicine, St. Louis, United States •
[2]Department of Medicine, Division of Oncology, Washington University School of Medicine, St. Louis, United States •
[3]Department of Cell Biology & Physiology, Washington University School of Medicine, St. Louis, United States •
[4]Department of Neuroscience, Washington University School of Medicine, St. Louis, United States

eLife Assessment

This is an **important** study that develops multiple human iPSC-based models to study the consequences of DNMT3A mutations in Tatton-Brown-Rahman Syndrome. **Convincing** evidence shows dysregulation of GABAergic interneuron development and function, and the authors identify some of the key signaling mechanisms underlying these changes. This study will be of interest for understanding the functions of DNMT3A in brain development and the causes of neurological dysfunction in Tatton-Brown-Rahman Syndrome.

https://doi.org/10.7554/eLife.111056.1.sa4

Abstract

Pathogenic mutations in DNMT3A cause Tatton-Brown-Rahman Syndrome (TBRS), a disorder characterized by somatic overgrowth of multiple tissues including the brain and intellectual disability (OGID). Here, we investigated TBRS etiology using new human pluripotent stem cell models, modeling varying levels of TBRS-associated loss of DNMT3A function. We identified lineage-specific overgrowth in TBRS ventral forebrain medial ganglionic eminence (MGE)-like progenitors, due in part to increased signaling through the PIK3/AKT/mTOR pathway that could be modulated to ameliorate this phenotype. By contrast, reduced DNA methylation during MGE-like progenitor differentiation into GABAergic interneurons caused premature expression of neuronal and synaptic genes, triggering precocious neuronal maturation. As a result, TBRS GABAergic neurons exhibited sufficient hyperactivity to alter the development and structure of neuronal networks, likely contributing to the intellectual disability and autism spectrum disorder common to TBRS patients. Together, this work elucidates new roles for DNMT3A-mediated gene repression in human cortical development, identifying critical requirements for regulating GABAergic neuron production and neuronal network function. These findings also provide evidence for interrelated pathogenic mechanisms underlying TBRS and other OGIDs, including PIK3CA-related overgrowth syndrome and Weaver Syndrome, providing a foundation and rationale for future studies to identify common paradigms to treat these related disorders.

Introduction

Overgrowth and intellectual disability disorders (OGIDs) are a group of rare neurodevelopmental disorders (Atterton et al. 2025) often caused by mutations either in proteins that mediate epigenetic regulation or in components of the PI3K/AKT/mTOR signaling cascade (Tatton-Brown et al. 2017). Characteristic of this, mutations in the *de novo* DNA methyltransferase *DNMT3A* cause Tatton-Brown-Rahman Syndrome (TBRS), a neurodevelopmental disorder involving autism spectrum disorder (ASD), brain overgrowth, and intellectual disability (Ostrowski and Tatton-Brown 1993; Tatton-Brown et al. 2018; Lane et al. 2020; Thomas et al. 2024). Several TBRS-associated mutations have been identified, each of which causes distinct levels of DNMT3A loss of function (Smith et al. 2021), with a majority involving heterozygous missense mutations in functional domains of *DNMT3A*, while other classes of mutation occur more rarely (Tatton-Brown et al. 2018).

Expression data from human postmortem (Kang et al. 2011) and mouse brain samples (Feng et al. 2005) show that DNMT3A expression begins during mid to late gestation, overtaking DNMT3B as the predominant *de novo* methyltransferase during early mouse neurodevelopment (Watanabe et al. 2006), where it regulates neural progenitor differentiation (Wu et al. 2012). However, despite the presence of DNMT3A during mouse brain development, TBRS mouse models exhibit anatomical and behavioral deficits reminiscent of TBRS with no evidence for brain overgrowth (Christian et al. 2020; Smith et al. 2021; Beard et al. 2023). Additionally, as these TBRS modelling efforts have focused on postnatal development to date (Christian et al. 2020; Smith et al. 2021; Beard et al. 2023), assessing how TBRS-associated loss of DNMT3A function alters early neurodevelopment to contribute to TBRS etiology remains critical. Furthermore, while the etiology of several other OGID disorders also remains understudied particularly in human models, recent evidence supports a requirement for *EZH2*, another OGID-associated gene, in restraining human neuronal differentiation (Ciceri et al. 2024), while evidence from mouse models suggest that EZH2 and DNMT3A function may be interrelated (Li et al. 2022). Therefore, investigating TBRS-associated cellular etiology and testing whether convergent molecular mechanisms contribute to other forms of OGID builds an essential foundation for developing both TBRS-specific and shared interventions across OGIDs.

Here we derived new pluripotent stem cell (hPSC) models of TBRS and studied how *DNMT3A* loss of function (LOF) mutations alter key aspects of human cortical development. TBRS models showed increased progenitor proliferation specific to medial ganglionic eminence (MGE)-like ventral forebrain neuronal progenitors (V-NPCs) associated with increased signaling through the PIK3/AKT/mTOR pathway. TBRS models also exhibited increased neurogenesis and neuronal maturation in both 2-D and 3-D models of GABAergic interneuron development, correlating with precocious neuronal gene expression resulting from reduced DNA methylation. This resulted in GABAergic neuron hyperactivity sufficient to disrupt neuronal network synchrony. Together, this work demonstrates that GABAergic neurons are particularly sensitive to TBRS-associated DNMT3A mutation and also identifies convergent mechanisms associated with dysregulation across related OGID genes.

Results

TBRS models show increased V-NPC proliferation and mTOR signaling

To study the impact of TBRS-associated mutations on neuronal development and function we established four new sets of TBRS models spanning different levels of DNMT3A loss of function (LOF), consistent with the range of DNMT3A LOF observed across TBRS patient alleles (Nguyen et al. 2019; Christian et al. 2020; Smith et al. 2021; Beard et al. 2023). These included an induced pluripotent stem cell (iPSC) model from a patient with a p.R882H mutation (882), a recurrent severe loss of function (LOF) variant that we corrected to generate an isogenic control (C-WT, Fig. 1a), a human embryonic stem cell (hESC) model (WT) with variant knock-in of a

p.P904L mutation (904), and an hESC model carrying small deletions near the end of the gene in both DNMT3A alleles and predicted to disrupt methyltransferase function (KO, Fig. 1b). We also derived two additional iPSC models from a patient with full gene deletion of one DNMT3A allele (Del1/2), which we paired with two unrelated sex matched control iPSC models from neurotypical individuals (Con1/2, Fig. 1c). Finally, we established two CRISPRi DNMT3A knockdown models (G1/G2) with their isogenic control (KRAB) (Fig. 1d). Total DNMT3A protein levels across these human pluripotent stem cell models (hPSCs) demonstrate little change in the 882 or 904 models, as expected (Fig. 1e-f), but significant loss of DNMT3A protein in the KO, Del1/2, and G1/G2 models (Fig. 1f-h).

As brain overgrowth is central to TBRS clinical presentation, we first assessed whether these TBRS models exhibited altered growth during specification of neural progenitor cells (NPCs) with a dorsal (D-, Fig. 1i) or ventral (V-, Fig. 1j) telencephalic character. Initial observations highlighted an increase in neurosphere outgrowth in V-NPCs but not D-NPCs across the 882, 904 and Del1 models (Fig. 1k-l, Supplemental Fig. S1a-d). Further quantification of Ki67+ cells substantiated increased proliferation specific to V-NPCs across these TBRS models (Fig. 1m-o, Supplemental Fig. S1e-g) while assessments of lineage specific markers (PAX6 in D-NPCs or NKX2.1 in V-NPCs) showed no significant difference between control and TBRS NPCs (Supplemental Fig. S1h-m). Similar assessments in KO, Del2, and CRISPRi (G1/G2) V-NPCs also highlighted increased proliferation specific to V-NPCs (Fig. 1p, Supplemental Fig. S2a-d), solidifying this as a core TBRS-related phenotype.

As mutations in PI3K/AKT/mTOR pathway genes also cause an OGID disorder (PIK3CA-related overgrowth syndrome, PROS) and this pathway is an established regulator of NPC proliferation (Romanyuk et al. 2024), we next assessed if signaling through this pathway was altered in TBRS V-NPCs, finding that expression and/or phosphorylation of AKT3, mTOR and the mTOR target, ribosomal protein S6, increased specifically and consistently across TBRS V-NPCs (Fig. 1q-r, Supplemental Fig. S3a-d). This confirmed that increased PI3K/AKT signaling was associated with increased V-NPC proliferation. We further tested whether reducing mTOR activity could correct TBRS-associated increases in V-NPC proliferation, demonstrating that rapamycin treatment significantly reduced V-NPC proliferation in TBRS models (Fig. 1s, Supplemental Fig. S3e-f). Together, these results highlight V-NPCs as highly sensitive to TBRS mutation, while also linking DNMT3A LOF with signaling disruptions underlying PROS, suggesting that convergent molecular mechanisms underlie brain overgrowth across genetically distinct OGID disorders.

DNMT3A restrains the onset of neuronal gene expression during V-NPC specification

To define molecular mechanisms disrupted by TBRS mutation in NPCs, we profiled gene expression changes between TBRS (882 and 904) and control V-NPCs, finding both distinct and shared effects across TBRS models (Fig. 2a-b, Supplemental Data 2). Focusing on differentially expressed genes (DEGs) that were similarly dysregulated in both models (shared-DEGs, Fig. 2b, Supplemental Data 2) we found the majority were up-regulated in TBRS models (Fig. 2b, Supplemental Data 2) and generally showed a greater effect size in 882 versus 904 V-NPCs (Supplemental Fig. S4a, Supplemental Data 2). While some of the shared-DEGs up-regulated in TBRS models encoded regulators of cell proliferation, consistent with the V-NPC overgrowth we observed, the majority were genes associated with neuronal differentiation (Fig. 2c, Supplemental Data 3), suggesting a second core function for DNMT3A. Assessing the expression of 30 of these shared-DEGs in 882 (severe LOF), 904 (mild LOF), G2 (mild LOF), and G1 (mildest LOF) V-NPCs, we found that increased expression of these genes correlated with DNMT3A LOF severity (Fig. 2d, Supplemental Fig. S4b), confirming a substantive role for DNMT3A in regulating both proliferative and neuronal gene expression. However, despite this substantive increase in neuronal gene expression, TBRS V-NPCs retained a progenitor identity (Supplemental Fig. S4c, Supplemental Data 2), signifying that DNMT3A LOF alone was insufficient to initiate

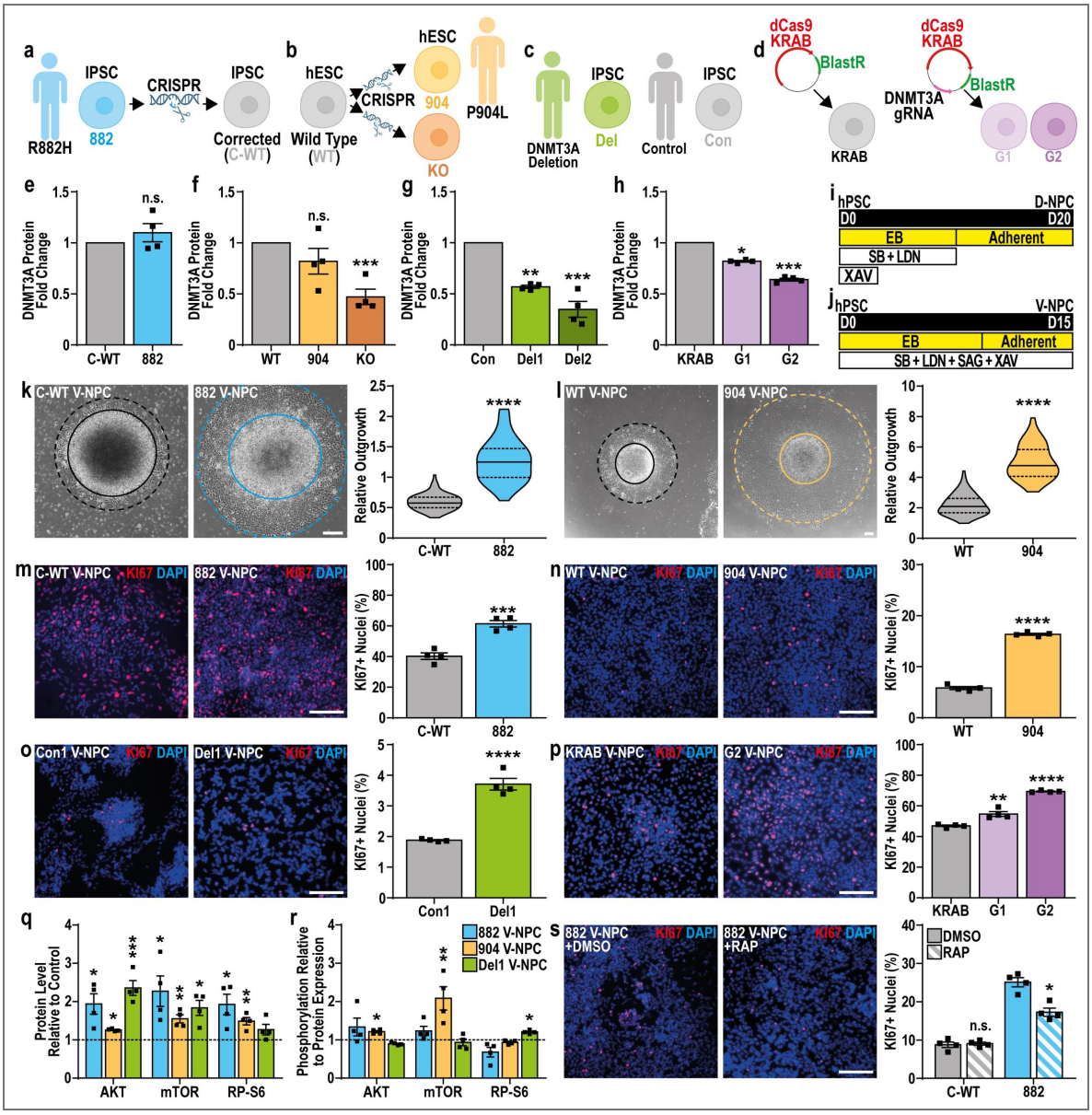

Fig. 1. TBRS models show increased V-NPC proliferation and mTOR signaling.

a, iPSCs carrying a p.R882H mutation in DNMT3A (882), generated from a TBRS patient and corrected to generate an isogenic control (C-WT). **b,** Control hESCs (WT), modified to mimic a TBRS patient with heterozygous p.P904Lmutation (904) via knock-in, which also created a model with small <10 bp mutations in both DNMT3Aalleles (KO). **c,** Two clonal iPSC lines were generated from a TBRS patient with heterozygous deletion of the DNMT3Agene (Del1/2) and compared with sex-matched unrelated control iPSCs (Con1/2). **d,** CRISPRi hPSC models were generated using two gRNAs targeting DNMT3A (G1/2) and compared with hPSCs without gRNA (KRAB). **e-h,** Quantification of DNMT3A protein expression in **(e)** 882, (f) 904, (f) KO, **(g)** Del1/2, and **(h)** G1/2 TBRS models versus matched controls. **i-j,** Schematic representation of (i) D-NPC specification and U) V-NPC specification. **k-I,** Representative images and quantification of relative neurosphere outgrowth (dotted line) from plated neurospheres (bold line) at D12 of **(k)** 822 and **(1)** 904 V-NPC specification versus matched controls. **m-p,** Representative images and quantification of Kl67 immunopositivity in **(m)** 822, **(n)** 904, **(o)** Del1 and **(p)** G1/2 V-NPCs versus matched controls. **q-r,** Quantification of relative **(q)** abundance and **(r)** phosphorylation of AKT, mTOR, and ribosomal protein S6 in TBRS V-NPCs (882, 904 and DeI1) versus matched controls (dotted line). **s,** Representative images and quantification of Kl67 positivity in 882 and C-WT V-NPCs after treatment with rapamycin (RAP) or vehicle control (DMSO). Data is represented as mean +/- SEM **(e-h,m-s)** or as distributions, with median (bold line) and upper and lower quartiles (dotted lines) indicated **(k-I),** and analyzed by Students I-test, versus matched controls **(e-h,k-s).** n=4 biological replicate experiments for all conditions, pValues: *p<0.05;**p<0.01;***p<0.001;****p<0.0001. Scale bars=200 µm **(k-I)** and 100 µm **(m-p,s).**

neuronal differentiation. By contrast, parallel transcriptomic assessments of 882 D-NPCs revealed little effect of DNMT3A LOF mutation on gene expression, consistent with the lack of cellular phenotypes observed in TBRS D-NPCs (Supplemental Fig. S4d, Supplemental Data 2).

We next investigated the proximal cause of the TBRS-associated transcriptomic dysregulation by identifying changes in DNA methylation (mCG) in 882 and 904 V-NPCs, identifying significant global and regional mCG decreases specific to 882 V-NPCs (Fig. 2e; Supplemental Fig. S5a). Focusing on the 882 model, we identified differentially methylated regions (DMRs), most of which lost mCG in 882 V-NPCs (hypo-DMRs, Supplemental Data 4), with these sites commonly associated with synaptic and neuronal genes upregulated in TBRS V-NPCs (Fig. 2f-g, Supplemental Data 5). Examining mCG changes in both 882 and 904 V-NPCs, we found 882 V-NPCs exhibited greater mCG loss than 904 V-NPCs across the superset of all DMRs present in both TBRS models (All DMRs, Fig. 2h) and at 882 hypo-DMRs (Fig. 2h), consistent with differential DNMT3A LOF across these models. When examining the subset of DMRs consistently hypo-methylated across both TBRS models, we found a similar reduction in mCG levels across both models (Fig. 2h). Furthermore, these shared-DMRs were often located at gene promoters (Supplemental Fig. S5b) of neuronal genes (Fig. 2i, Supplemental Data 5), many of which were also shared-DEGs (Supplemental Data 5). Parallel analyses in 882 D-NPCs also revealed substantive changes in mCG (Supplemental Data 4), but these changes did not correlate with substantive transcriptomic changes. Together, these results demonstrate that TBRS-associated mutations disrupt the ability of DNMT3A to restrain the onset of neuronal gene expression during V-NPC specification.

TBRS organoids modeling ventral forebrain development exhibit increased neurogenesis

To examine the consequences of TBRS-associated alterations on NPC development, we profiled changes in the development of dorsally (D-ORG, Fig. 3a) and ventrally (V-ORG, Fig. 3b) patterned forebrain-like organoids. Drawing comparisons with the increased proliferation observed in our 2-D V-NPC derivation scheme, we found the proliferative Ki67+ cell fraction likewise increased in TBRS (882, 904, and Del1) V-ORGs (Fig. 3c, Supplementary Fig. S6a), while assessing the V-NPC markers DLX2 and NKX2.1 revealed no consistent alterations in TBRS V-ORG specification (Supplementary Fig. S6b-c). Given the increased neuronal gene expression observed in TBRS V-NPCs, we also examined altered neurogenesis in TBRS V-ORGs, finding a significant increase in the TUJ1-immunopositive area (Fig. 3d-e), which was not due to loss of SOX2+ progenitors (Fig. 3d, f-g). Therefore, to assess whether this increase in TUJ1-immunopositive area resulted from increased neurogenesis, we also examined the proportion of cells positive for the pro-neurogenic marker ASCL1 or immature GABAergic neuron marker SST, finding an increase in both ASCL1+ and SST+ cells in TBRS V-ORGs (Fig. 3h-i, Supplementary Fig. S6d-e), substantiating an increased neurogenesis in TBRS V-ORGs.

Performing similar assessments in D-ORGs, we found no consistent evidence for altered proliferation (Supplemental Fig. S7a), again congruent with our prior observations in 2-D models. However, we did observe an increased proportion of SOX2+ cells in 904 D-ORGs with no significant change in the TUJ1 immunopositive region across TBRS D-ORGs (Supplementary Fig. S7b-c). Finally, we assessed changes in neurogenesis using ASCL1, the radial glial cell marker TBR2, and the early born cortical glutamatergic neuron marker TBR1, finding no consistent differences in the proportion of any of these populations in TBRS D-ORGs (Supplementary Fig. S7d-f). Therefore, consistent with our findings in 2-D models of NPC specification, our organoid models also show that TBRS-associated DNMT3A LOF has little effect on D-NPC development, while causing increased proliferation and neurogenesis during V-NPC development, suggestive of increased production and/or maturation of GABAergic neurons.

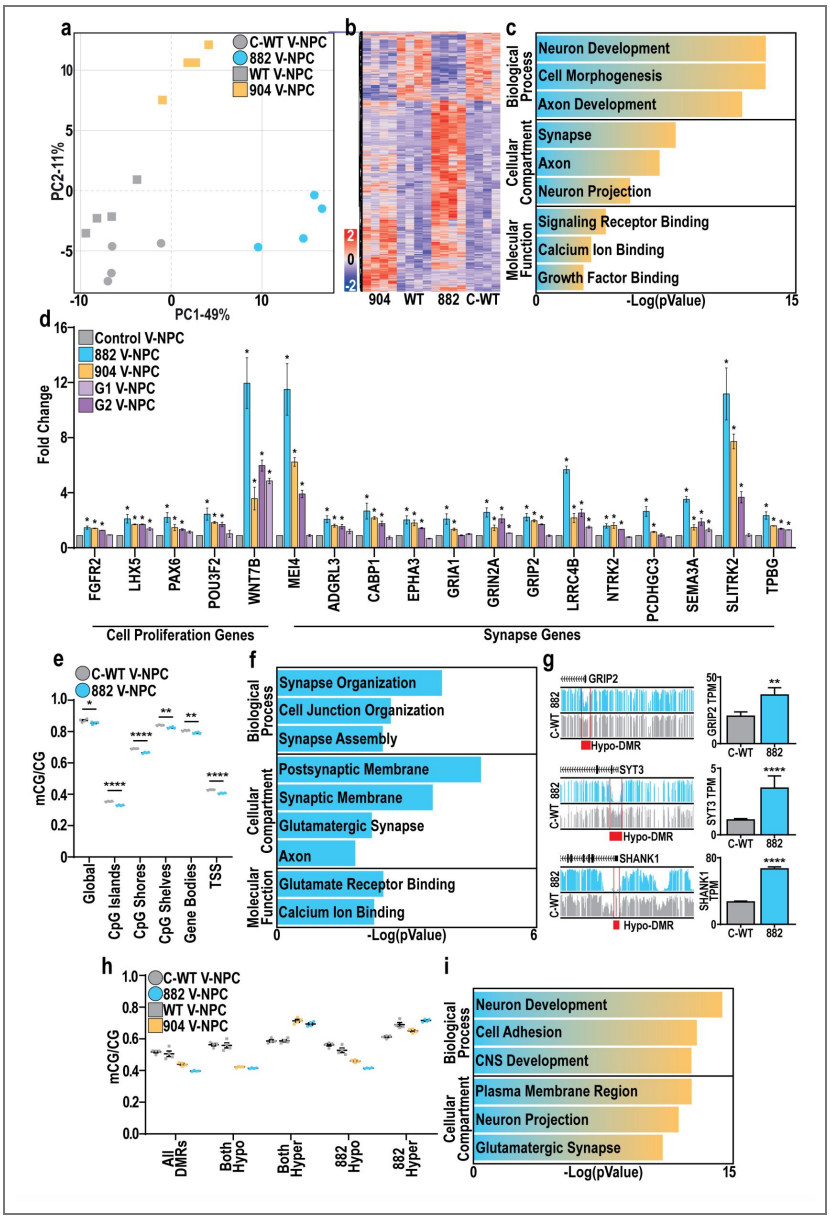

Fig. 2. DNMT3A mediates epigenetic repression of pro-neuronal genes in V-NPCs

a, Principal component analysis of control (grey) and TBRS (882-blue and 904-orange) V-NPCs. **b,** Heatmap of shared DEGs across both 882 and 904 versus control (C-WT/WT) V-NPCs. **c,** Summary of GO enrichment analysis of DEGs upregulated in TBRS (882/904) versus control V-NPCs. **d,** Expression changes of genes associated with 'cell proliferation' and 'synapse' GO terms across TBRS (882, 904, G1/2) versus control V-NPCs. **e,** Changes in mCG/CG levels in C-WT versus 882 V-NPCs. **f,** Summary of GO enrichment analysis of 882 DEGs associated with an 882 hypo-DMR. **g,** Genomic browser views of mCG in C-WT and 882 V-NPCs, highlighting hypo-DMRs (red) associated with promoters of DEGs upregulated in 882 V-NPCs. **h,** mCG/CG differences at shared-DMRs (All), qualified by directionality of DMRs in both TBRS models (both-hyper or both-hypo) or specifically in the 882 model (882-hyper or 882-hypo). i, Summary of GO enrichment analysis of DEGs upregulated in TBRS (904 and 882) V-NPCs and associated with shared hypo-DMRs.Data is represented as mean +/-SEM **(d,e,g,h)** with individual biological replicates indicated **(e,h).** Data was analyzed by Student's t-test versus isogenic controls **(d,e)** or by differential expression analysis **(g).** n=4 biological replicate experiments for all conditions, pValues: *p<0.05 **(d)** and *p<0.05; **p<0.01; ****p<0.0001**(e,g).**

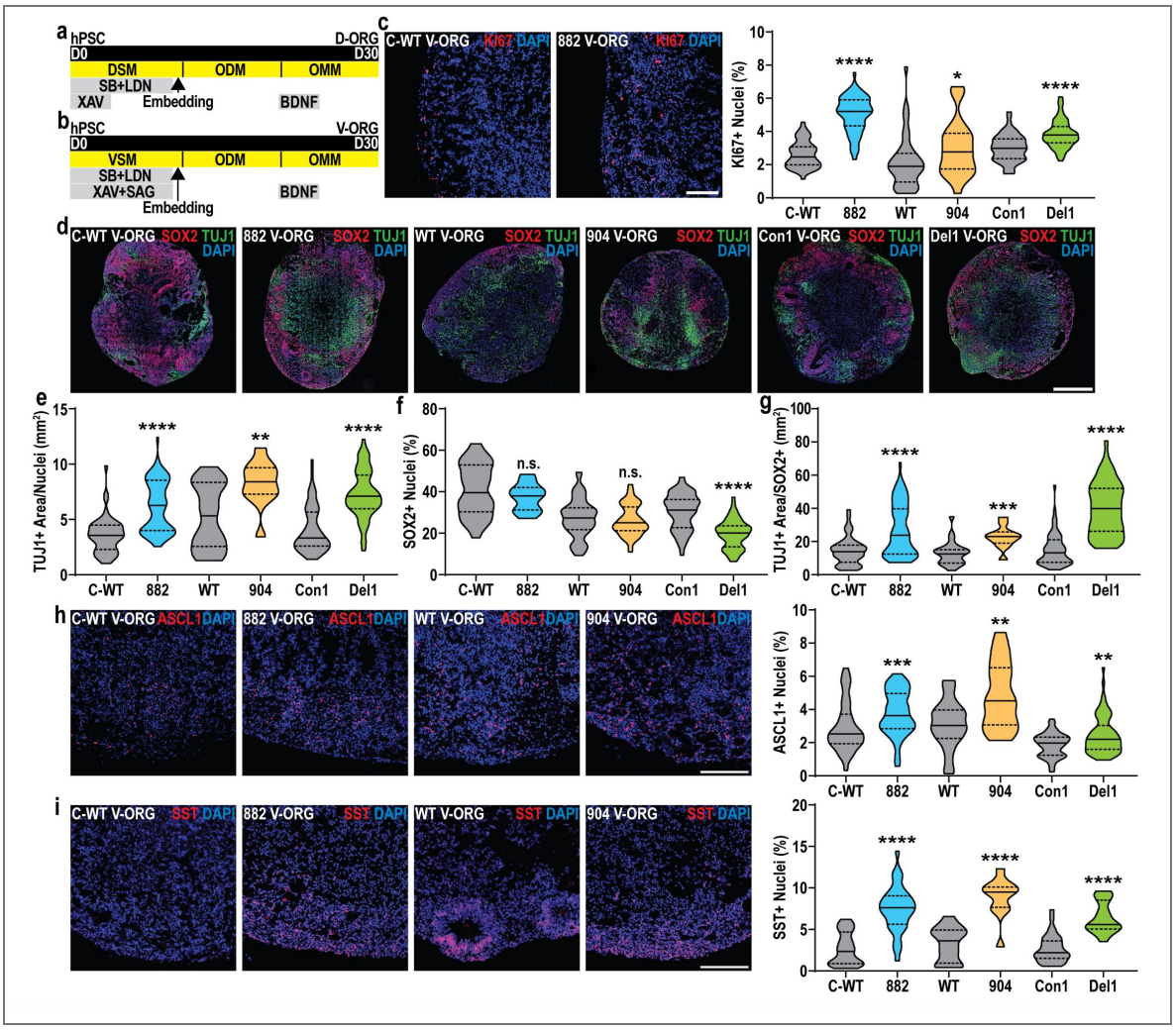

Fig. 3. TBRS V-ORGs show increased proliferation and neurogenesis.

a-b, Schematic representation of **(a)** D-ORG or **(b)** V-ORG differentiation. **c,** Representative images and quantification of KI67+ cell fraction across TBRS and control V-ORGs. **d-g,** Representative images of **(d)** SOX2 and TUJ1 staining in TBRS and control V-ORGs, alongside quantification of **(e)** TUJ1+ area, **(f)** SOX2+ fraction (% of DAPI+ nuclei) and **(g)** TUJ1+ area normalized to SOX2+ cells. **h-i,** Representative images and quantification of the **(h)** ASCL1+ and (i) SST+ cell fraction across TBRS and control V-ORGs. All data is represented as distributions with median (bold line) and upper and lower quartiles (dotted lines) indicated and was analyzed by Mann-Whitney tests, comparing each TBRS model to its matched control. A minimum of 3 batches of organoids were prepared for each condition, with 3-9 organoids assessed per batch. pValues: *p<0.05; **p<0.01; ***p<0.001; ****p<0.0001; n.s.-non-significant. Scale bars=100 μm **(c,h-i)** and 500 μm (d).

Repressive H3K27me3 compensates for severe loss of DNA methylation

Prior work has also demonstrated a role for *EZH2* in restraining neuronal maturation during human glutamatergic neuron differentiation, a particular interest as mutations in EZH2 are known to cause the OGID Weaver syndrome(Gibson et al. 2012; Tatton-Brown et al. 2013; Ciceri et al. 2024). As this was reminiscent of our findings for DNMT3A LOF mutation, we investigated if levels of histone H3 lysine 27 tri-methylation (H3K27me3) deposited by EZH2 were altered in our TBRS models. Identifying sites of differential H3K27me3 enrichment (DKSs) in both 882 D-NPCs and V-NPCs, we found that the majority gained H3K27me3 in the TBRS model (hyper-DKS, Fig. 4a-b, Supplemental Data 6). Interestingly, while D-NPC and V-NPC hyper-DKSs that intersected with 882 hypo-DMRs were associated with genes involved in early neural development (Fig. 4c-d, Supplemental Data 7), few of these were TBRS DEGs. Thus, we hypothesized that H3K27me3-mediated repression may compensate for mCG reduction in 882 NPCs, potentially preventing transcriptomic dysregulation due to DNMT3A LOF, particularly in D-NPCs where transcriptomic changes due to mCG hypomethylation are muted.

To test this hypothesis, we identified a set of genes in 882 D-NPCs that were associated both with hypo-DMRs and hyper-DKSs but were not TBRS DEGs (e.g. ESRG and ARX, Fig. 4e) and tested whether disrupting H3K27me3 deposition altered their expression. Either EZH2 knockdown in 882 TBRS D-NPCs using siRNAs (Fig. 4f, Supplemental Fig. S8a) or disruption of EZH2 activity with a selective chemical inhibitor (EZH2i) caused increased target gene expression relative to controls (Fig. 4g-h). Significantly, these effects were not observed in D-NPCs with less severe DNMT3A LOF (904; Supplemental Fig. S8b), suggesting that compensatory H3K27me3 increases may be triggered by the more severe mCG loss in the 882 model. Given these findings, we also tested whether EZH2 overexpression (OE) could reverse TBRS-associated increases in gene expression, finding that EZH2 OE partially rescued TBRS-associated transcriptomic dysregulation (Fig. 4i-j). Together, these results indicate that repressive H3K27me3 compensates for reduced DNA methylation stemming from severe mCG loss, while increased EZH2 activity can ameliorate some TBRS-associated molecular phenotypes. This suggests that DNMT3A and EZH2 regulate similar suites of genes and support an overlapping mechanism of pathogenicity between OGIDs TBRS and Weaver syndrome.

TBRS mutations cause precocious maturation of GABAergic neurons

We next investigated whether the elevated neuronal gene expression found in TBRS V-NPCs persisted upon their differentiation into immature GABAergic cortical interneurons (V-INs; Fig. 5a). Reminiscent of our V-NPC analysis, we identified greater transcriptomic differences in 882 than 904 V-INs (Fig. 5b, Supplemental Data 8), while shared-DEGs upregulated in TBRS V-INs were again enriched for synaptic genes (Fig. 5c, Supplemental Data 9). Effect sizes of TBRS V-IN shared-DEGs were likewise generally larger in 882 versus 904 V-INs, as exemplified by 42 synapse-associated shared-DEGs (Fig. 5d, Supplemental Data 9). We also performed comparative gene set enrichment analysis with published data from the adult cortex of a TBRS mouse model (p.R878H) analogous to the 882 human model (Beard et al. 2023), finding shared upregulation of neuronal and synaptic genes (Supplemental Data 10). Together, these results highlight substantive evidence for synaptic gene dysregulation as a core phenotype associated with TBRS mutation.

To establish if continued upregulation of these synaptic genes resulted from persistent mCG loss in TBRS V-INs, we examined DNA-methylation in 882 and 904 V-INs, highlighting milder mCG losses than those observed in V-NPCs (Supplemental Fig. S9a-b). However, identifying DMRs across TBRS V- INs highlighted many hypo-DMRs (Supplemental Data 11), with 904 V-IN hypo-DMRs frequently detected in 882 V-INs, but not vice versa (Fig. 5e, Supplemental Data 11). Focusing on hypo-DMRs shared across 882 and 904 V-INs (Fig. 5f, Supplemental Data 11) and associating these with V-IN shared-DEGs again revealed synaptic gene enrichment (Supplemental

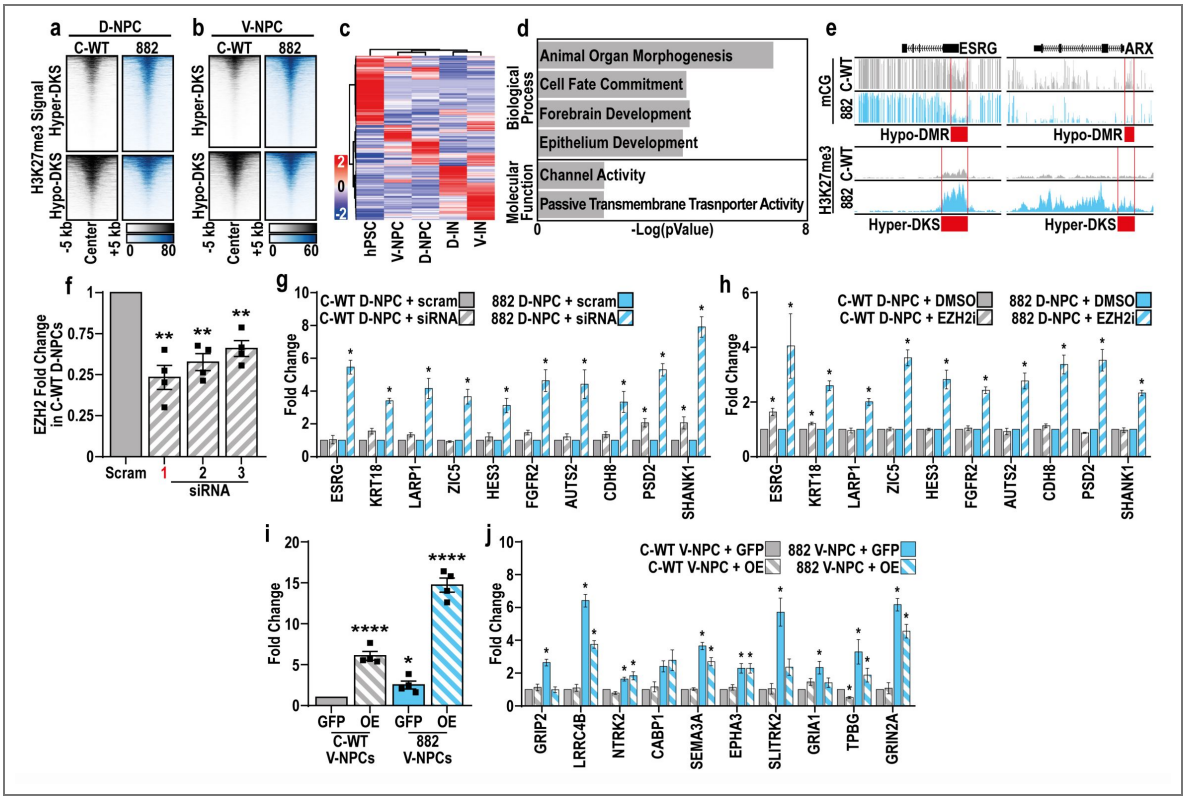

Fig. 4. Increased H3K27me3 compensates for loss of DNA methylation specifically in R882H NPCs.

a-b, H3K27me3 peaks with significantly increased (hyper-OKS) or decreased (hypo-OKS) enrichment in 882 versus control **(a)** D-NPCs or **(b)** V-NPCs.**c,** Expression of genes associated with hypo-DMRs and hypo-DKSs in 882 NPCs (D and V) across neuronal differentiations. **d,** Summary of GO enrichment analysis of non-DEGs associated with hypo-DMRs and hypo-DKSs in 882 NPCs (D and V). **e,** Genomic browser views of mCG and H3K27me3 in 882 and control V-NPCs, highlighting (red) hypo-DMRs and hyper-DKSs associated with promoters of two genes. **f,** Quantification of EZH2 mRNA levels in C-WT D-NPCs after treatment with either scrambled siRNA (scram) or siRNAs targeting EZH2 (1-3), highlighting selection of siRNA 1 for further study (red). **g-h,** Quantification of expression changes in 10 genes associated with 882 D-NPC hypo-DMRs and hyper-DKSs, after treatment with **(g)** siRNAs or **(h)** an EZH2-specific inhibitor. i, Quantification of EZH2 mRNA levels in C-WT and 882 V-NPCs after lentiviral transduction with a construct overexpressing either EZH2 (OE) or GFP (GFP). **j,** Quantification of expression changes in 10 genes upregulated in 882 V-NPCs under OE or GFP conditions. Data represented as mean+/-SEM **(f-j)** and was analyzed by one-way ANOVA, with comparison of treatment versus **(f-g)** scram,**(h)** DMSO or **(i-j)** GFP control treated conditions. n=4 biological replicate experiments for all conditions, pValues: *p<0.05; **p<0.01; ****p<0.0001 **(f,i)** or *p<0.05 **(g-h,j).**

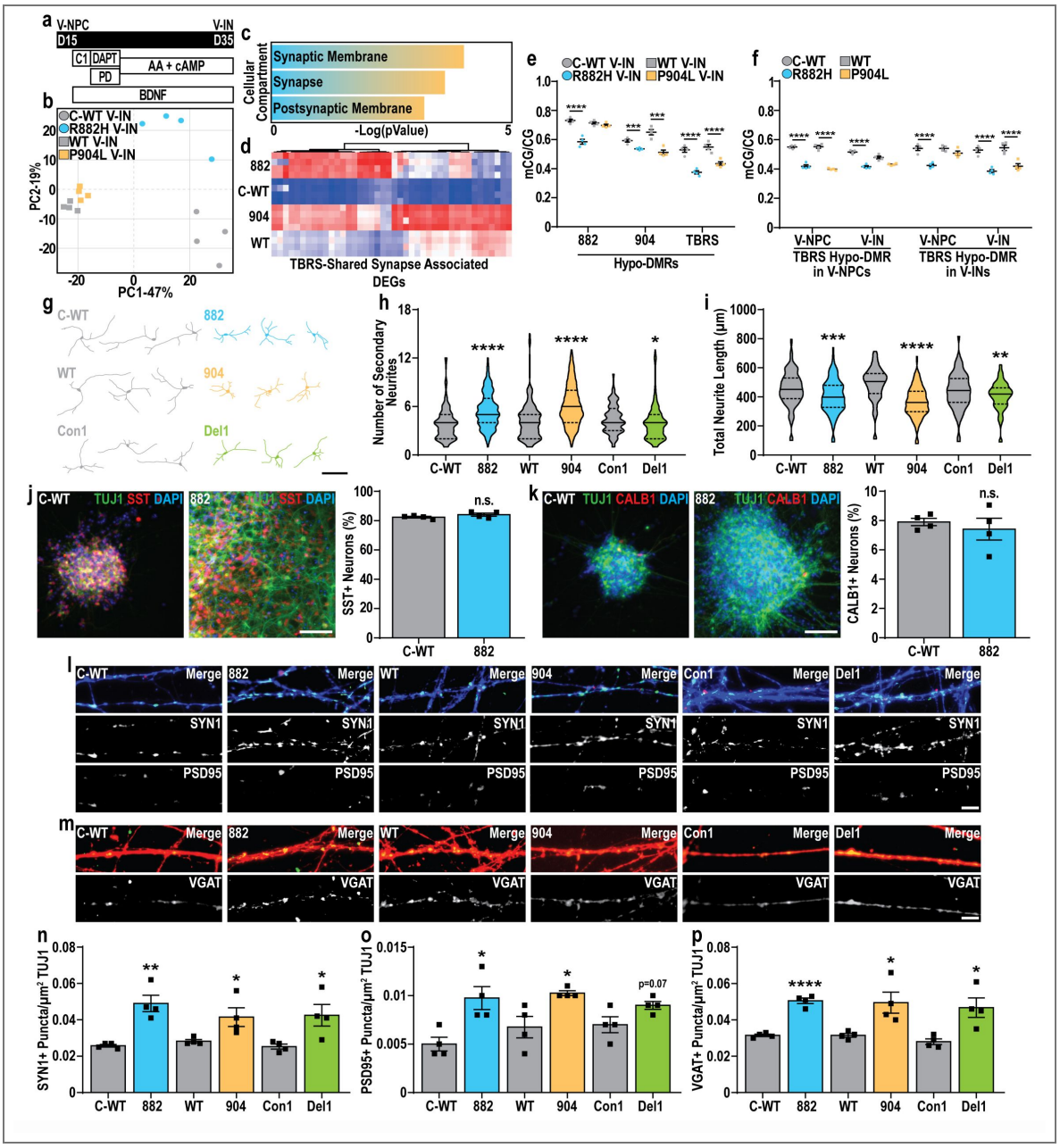

Fig 5. DNMT3A constrains neuronal maturation during interneuron differentiation.

a, Experimental paradigm for generating immature GABAergic neurons (V-INs) from ventrally patterned neuronal progenitors (V-NPCs). **b,** Principal component analysis of control (grey) and TBRS (882-blue and 904-orange) V-INs. **c,** Summary of GO enrichment analysis of DEGs upregulated in TBRS V-INs.**d,** Heatmap of genes associated with the 'synapse' GO term and upregulated in TBRS V-INs. **e,** Changes in mCG/CG at 882, 904, or shared (TBRS) V-IN hypo-DMRs and matched control V-INs. **f,** Changes in mCG/CG at TBRS-shared hypo-DMRs identified in V-NPCs or V-INs across both TBRS and control V-NPCs and V-INs. **g,** Representative example traces of control and TBRS D30 V-INs used to quantify neuronal morphology. **h-i,** Quantification of neuronal morphology in control and TBRS D30 V-INs, including **(h)** number of secondary neurites and (i) total neurite length. **j-k,** Representative images and quantification of the proportion of U) SST or **(k)** CALB1 positive neurons in day (D) 40 C-WT or 882 V-IN cultures. **1-p,** Representative images and quantification of pre-synaptic marker **(l,n)** SYN1 and postsynaptic marker **(1,o)** PSD95 puncta density, and **(m,p)** VGAT, across TBRS and control D50 V-INs. Data was analyzed by Students I-test versus matched controls **(e,f,h,i,n-p).** n=4 biological replicate experiments for all conditions with a minimum of 20 neurons quantified for morphological measures per biological replicate, pValues: *p<0.05;**p<0.01;***p<0.001;****p<0.0001. Scale bars=100 µm **(g),** 50 µm **U,k)** and 10 µm **(1,m).**

Data 9). We also found that, despite their similar association with synaptic genes, 882 hypo-DMRs persisted through development at the same sites, while locations of 904 hypo-DMRs were more temporally specific (Fig. 5f, Supplemental Data 11). Together, these findings support persistently diminished DNA methylation and concomitant upregulation of synaptic genes as a continued feature during TBRS GABAergic neuron differentiation.

To assess how these molecular phenotypes affected neuronal maturation, we next assessed whether TBRS GABAergic neurons exhibited altered morphology, scoring control and TBRS (882, 904, and Del1) V-INs at D30. This analysis revealed an increase in ramification, specifically involving increased secondary neurite production at the expensive of overall neurite length in TBRS V-INs (Fig. 5g-i, Supplemental Fig. S10a), while also highlighting an increase in soma size of TBRS V-INs (Supplemental Fig. S10b). We also assessed whether cortical interneuron identity was similarly disrupted by DNMT3A LOF by examining the production of CALB1+ and SST+ V-INs at day (D) 40, finding no significant difference in the immunopositive fraction for either marker in TBRS V-IN cultures (Fig. 5j-k, Supplemental Fig. S10c-f). Finally, we evaluated if synapse formation was disrupted in TBRS V-INs, finding increased synaptic marker density (SYN1, PSD95, and VGAT) in D50 TBRS V-INs (Fig. 5l-p). Together, these results confirm that TBRS-associated transcriptomic dysregulation during V-IN differentiation also causes premature V-IN maturation.

Performing parallel transcriptomic analysis in immature glutamatergic neurons (D-INs), we found substantive transcriptomic differences between TBRS (882 and 904) and control D-INs (Supplemental Fig. S11a-b), characterized by persistent expression of genes normally expressed in hPSCs and D-NPCs (Supplemental Fig. S11c-d, Supplemental Data 12-13). We tested whether this phenomenon was a consequence of altered development by bypassing NPC specification, instead deriving 882 and 904 glutamatergic-like neurons by inducible NGN2 overexpression (iGluts, Supplemental Fig. S11e); this revealed similar transcriptomic dysregulation across TBRS D-INs and iGluts (Supplemental Fig. S11f, Supplemental Data 12-13). We also found similar global losses of mCG across 882 but not 904 D-INs and iGluts (Supplemental Fig. S11g-j), while identifying DMRs in TBRS highlighted similar losses of mCG across D-INs and iGluts (Supplemental Fig. S11k; Supplemental Data 14). TBRS-shared hypo-DMRs in D-INs were often associated with neuronal and synaptic genes (Supplemental Data 13) and, consistent with this observation, we found DMRs across 882 D- and V-INs showed similar mCG losses (Supplemental Fig. S11l, Supplemental Data 13-14). Together, our work above shows that TBRS mutations profoundly alter GABAergic neuron development, due to persistent dysregulation of neuronal and synaptic gene expression, while TBRS glutamatergic neurons exhibit distinct transcriptomic changes largely decoupled from altered NPC specification and mCG loss.

TBRS associated GABAergic neuron dysfunction causes neuronal network hypersynchrony

We next assessed the functional consequences of TBRS mutation by performing patch clamp electrophysiology on glutamatergic or GABAergic neurons (matured D-INs or V-INs, respectively) plated in monoculture on rat astrocytes and further matured. Initial assessments showed no significant functional alterations in 882 glutamatergic neurons, consistent with the lack of cellular phenotypes during D-IN differentiation (Supplemental Fig. S12a-d, Supplemental Data 15). By contrast, 882 GABAergic neurons exhibited significant hyperactivity upon stimulation (Fig. 6a-b), without significant alterations to neuronal health (Fig. 6c, Supplemental Fig. S13a-d, Supplemental Data 16). This hyperactivity was characterized by an increased action potential (AP) amplitude and decreased AP halfwidth (Fig. 6d-e). We also observed increased sodium uptake, transient outward currents (TOC), and GABA responsiveness in 882 GABAergic neurons (Fig. 6f-h, Supplemental Fig. S13e). When similar data was generated for 904 glutamatergic or GABAergic neurons, combined, and analyzed, we likewise found evidence for neuronal hyperactivity upon stimulation (example in Fig. 6i, combined data in Fig. 6j), while neither neuronal cell type showed significant changes in other measures of neuronal health or activity (Supplemental Fig. S13f-k, Supplemental Data 15-16).

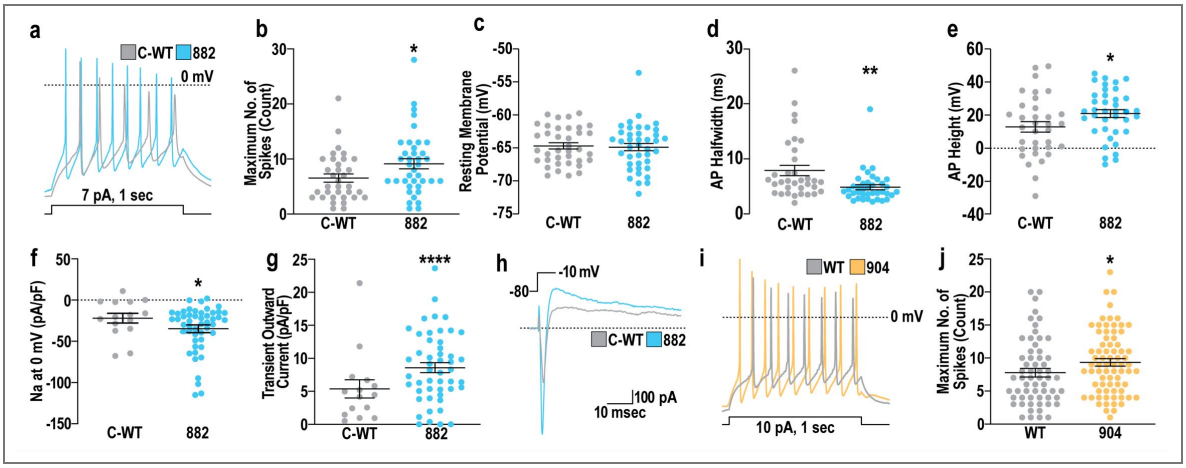

Fig 6. TBRS-associated mutations in DNMT3A cause GABAergic neuron hyperactivity.

a, Representative example traces of action potentials in C-WT (grey) or 882 (blue) GABAergic neurons induced by 1 second of stimulation. **b,** Quantification of maximum spike number across C-WT and 882 GABAergic neurons during 1 second of stimulation. **c,** Resting membrane potential of C-WT and 882 GABAergic neurons. **d-e,** Quantification of action potential (AP) characteristics, including **(d)** AP halfwidth and **(e)** AP height of C-WT and 882 GABAergic neurons. **f-g,** Measurements of (f) sodium (Na) current density at 0 mV and **(g)** transient outward current after voltage step, both normalized by capacitance (pA/pf).**h,** Example traces of current changes in C-WT and 882 GABAergic neurons during voltage step from -80 to -10 mV. **i,** Representative example traces of action potentials in WT (grey) or 904 (orange) GABAergic neurons induced by 1 second of stimulation. **j,** Quantification of maximum spike number, measured in both glutamatergic and GABAergic neurons (combined data analysis), during 1 second of stimulation. Significance was calculated by Rank Sum Test and results are presented as mean+/-SEM with data points representing measurements taken from individual neurons, *pValue<0.05;**pValue<0.01;***pValue<0.001.

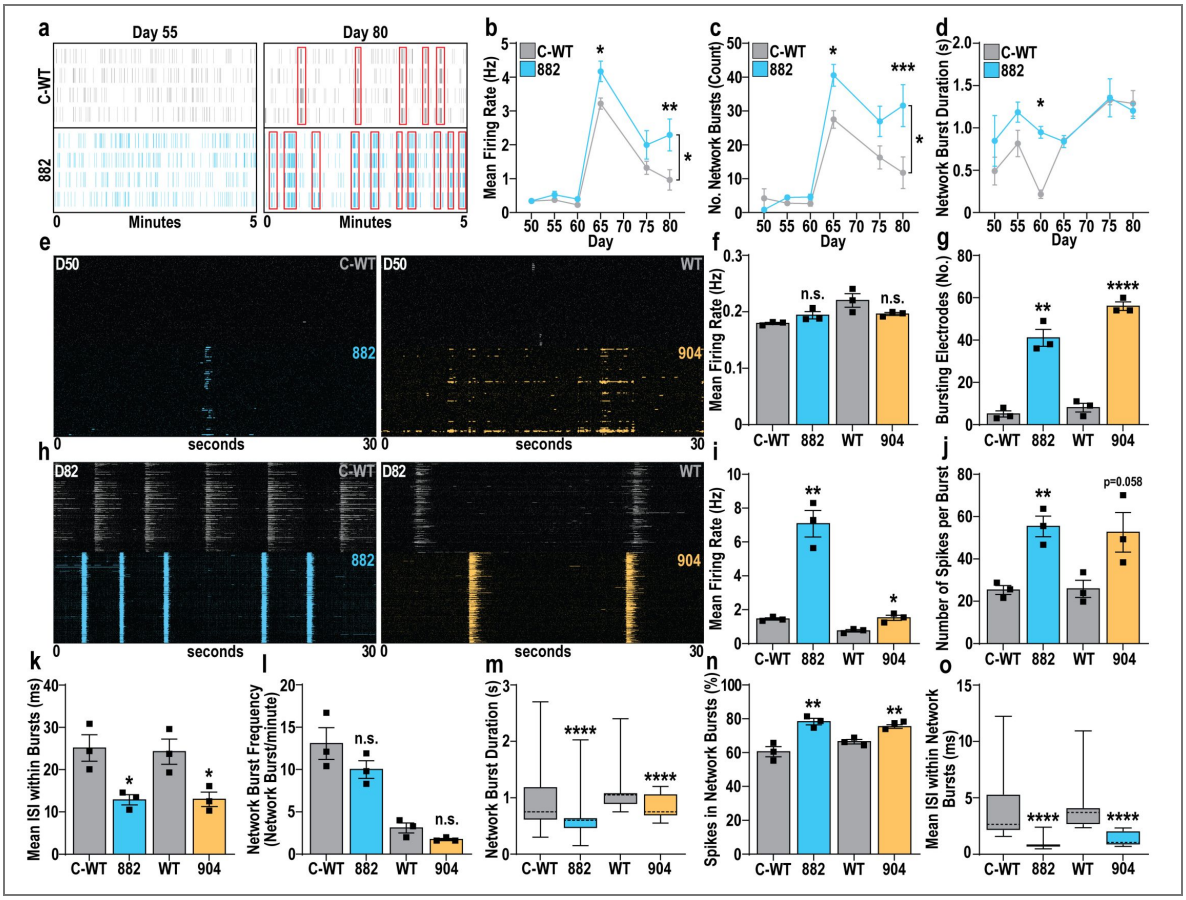

Fig 7. TBRS neuronal network dysfunction is driven by GABAergic neuron hyperactivity.

a, Representative raster plots of LD-MEA activity in C-WT or 882 GABAergic/glutamatergic neuron co-cultures from early (D55, left) to late (D80, right) time points, with synchronized activity indicated by red boxes. **b-d,** Characteristics of C-WT and 882 neuronal networks, highlighting increased **(b)** firing rate ($F_{1,6}$=6.579, pValue<0.05, n=4) and **(c)** frequency of network bursting ($F_{1,6}$=12.18, pValue<0.05,n=4) in 882 neuronal networks with no substantial changes in **(d)** network burst duration. **e-g,** Representative raster plots of HD-MEA activity **(e)** assessing the contribution of TBRS GABAergic neurons to neuronal network dysfunction after 50 days of differentiation, highlighting effects of TBRS GABAergic neurons on (f) firing rate and **(g)** appearance of neuronal bursting activity. **h-o,** HD-MEA activity assessing the contribution of TBRS GABAergic neurons to neuronal network dysfunction after 82 days of differentiation. **h-i,** Representative raster plots and quantification of changes in firing rate in cultures containing TBRS GABAergic neurons. **j-k,** Characterization of neuronal bursting parameters altered by TBRS GABAergic neurons, including U) the number of spikes per burst and the **(k)** inter-spike-interval (ISI) between spikes within neuronal bursts. **1-o,** Characterization of neuronal network parameters altered in the presence of TBRS GABAergic neurons, including network burst (I) frequency and **(m)** duration alongside the **(n)** proportion of activity within network bursts and the **(o)** ISi of spikes within network bursts. Data was analyzed by: two-way ANOVA, with posthoc Tukey's multiple comparison testing **(b-d),** Student's t-test **(f,g,i,j,k,l,n)** or Mann-Whitney test **(m,o),** versus isogenic controls. Data is represented as mean+/-SEM **(b-d,f,g,i,j,k,l,n)** with data points representing individual biological replicates **(f,g,i,j,k,l,n)** or as box-whisker plots with means indicated with dotted lines **(m,o).** For all experiments n=3 biological replicates; *pValue<0.05; **pValue<0.01; ***pValue<0.001;****pValue<0.0001; n.s.=not significant.

We next used low density (LD) multi-electrode arrays (MEAs) to assess changes in neuronal network activity in co-cultures of control or TBRS glutamatergic and GABAergic neurons. This analysis showed divergent results across models, with 882 cultures showing increased activity (Fig. 6k-n; Supplemental Fig. S14a-b), while trends from 904 cultures were inconsistent with this finding (Supplemental Fig. S14c-g). Therefore, to study these phenotypes at greater resolution, we assessed neuronal network activity using high density (HD) MEAs, focusing on TBRS GABAergic neuron dysfunction. Examining TBRS or control day (D) 50 GABAergic neurons co-cultured with control iGluts, we observed no differences in mean firing rate (MFR) but increased numbers of electrodes exhibiting bursting behavior (Fig. 6o-q). Furthermore, in assessing the same cultures at D82, co-cultures containing TBRS GABAergic neurons had an increased MFR, with a greater effect size in cultures containing 882 versus 904 GABAergic neurons (Fig. 6r-s). This was coupled with a decreased inter-spike interval (ISI) and increased coefficient of variation (CoV) of ISI associated with both the 882 and 904 models, with cultures containing GABAergic 882 neurons again showing greater effect sizes (Supplemental Fig. S15a-b).

Given the importance of GABAergic neurons in synchronizing neuronal activity (Makinen et al. 2018; Kirmse and Zhang 2022), we further investigated changes in neuronal bursting and neuronal network activity in these D82 co-cultures. This analysis highlighted decreased AP height (Supplemental Fig. S15c-e) in bursting neurons and increased numbers of spikes per burst (Fig. 6t), in cultures containing TBRS GABAergic neurons. Furthermore, cultures with 882 GABAergic neurons showed both increased bursting frequency (Supplemental Fig. S15f) and proportion of spikes in bursts with decreased inter-spike interval (ISI) within bursts (Fig. 6u, Supplemental Fig. S15g). Finally, while we did not observe alterations in the frequency of neuronal network activity associated with either TBRS model (Fig. 6v), TBRS GABAergic neurons caused a decreased duration of network bursts (Fig. 6w), coupled with increased numbers and proportions of spikes within network bursts (Fig. 6x, Supplemental Fig. S15h). These alterations were accompanied by decreased ISI and increased ISI coefficient of variation (CoV) of spikes within network bursts (Fig. 6y, Supplemental Fig. S15i). Together, these data demonstrate that both 882 and 904 TBRS-associated GABAergic neuron dysfunction is sufficient to drive neuronal network hyper-synchrony.

Discussion

In this work, we derived new human models of TBRS and used these to characterize TBRS-associated alterations of neurodevelopment and neuronal function, identifying GABAergic neuron development as selectively sensitive to pathogenic *DNMT3A* mutation. We identified critical functions for DNMT3A in restraining both proliferation and neurogenesis during GABAergic neurodevelopment. We demonstrated that disruption of DNA methylation in TBRS models causes premature expression of neuronal and synaptic genes during GABAergic neuron differentiation, driving GABAergic neurogenesis and, ultimately, neuronal hyperactivity. This GABAergic neuron hyperactivity is sufficient to disrupt neuronal network formation, causing neuronal network hyper-synchronicity. Finally, we highlight mechanistic links between TBRS and other OGIDs caused by mutations in other epigenetic modifiers and in the PIK3/AKT/mTOR signaling axis. Together, these findings reveal new developmental and lineage-specific roles for DNMT3A likely to underlie TBRS pathogenesis.

Significantly, the differential extent of TBRS-associated LOF in our models correlated with phenotypic severity, reminiscent of findings from the 882 and 904 orthologous TBRS mouse models (Smith et al. 2021; Beard et al. 2023). However, murine TBRS studies to date have focused on non-CG methylation catalyzed by DNMT3A in post-mitotic neurons of adult animals (Christian et al. 2020; Beard et al. 2023), while we instead found that aberrant development of GABAergic neurons underlies neuronal network hyperactivity and hypersynchrony in human TBRS models. Similarly, DNMT3A homozygous knockout during human motor neuron (hMN) development altered hMN function, causing hyperactivity; however, this was accompanied by impaired neurogenesis and synapse production (Ziller et al. 2018), counter to our findings. Our findings instead demonstrate a role for DNMT3A in restraining cortical neuron maturation, defining

distinct cell-type specific consequences of DNMT3A disruption by TBRS mutation. We also identified hyperproliferation specific to GABAergic neuron specification across TBRS models, which may contribute to the brain overgrowth in TBRS patients. Given the lack of brain overgrowth reported in murine models of TBRS (Christian et al. 2020; Beard et al. 2023), our work suggests that this may be a human specific phenomenon, consistent with findings for several other neurodevelopmental disorders (Ernst 2016; Marchetto et al. 2017; Wang et al. 2020; Connacher et al. 2022). Our results also support functional interplay between TBRS and PROS, with TBRS models showing increased PIK3/AKT/mTOR signaling, consistent with the finding that gain of function mutations in components of this pathway cause the related brain overgrowth disorder PROS (Mirzaa et al. 2016). While PROS-associated mutations remain understudied (Mirzaa et al. 2016; Dobyns and Mirzaa 2019) this signaling axis promotes excessive proliferation in the context of cancer (Samuels et al. 2005; Wang et al. 2017; Chen et al. 2022), such that pharmacological modifiers of PIK3/AKT/mTOR signaling are widely available. While our work highlighted the use of rapamycin in modulating hyperproliferation, prior studies have used other modulators of this signaling axis to rescue neuronal network abnormalities associated with TSC deficiency (Alsaqati et al. 2020), which likewise disrupts GABAergic neuron differentiation (Fu et al. 2012) and function (Bassetti et al. 2021). Therefore, if altered PIK3/AKT/mTOR signaling is a common hallmark across OGIDs as our data suggests, this may present an opportunity for synergistic intervention to treat multiple genetically distinct OGIDs.

Our findings also support mechanistic interplay between EZH2 and DNMT3A in restraining human GABAergic neuron differentiation, suggesting a common mechanism may underlie etiology of both TBRS and Weaver syndrome, an OGID caused by *EZH2* mutations (Tatton-Brown et al. 2013; Cohen et al. 2016; Tatton-Brown et al. 2017). Recent work demonstrated a role for EZH2 in restraining glutamatergic neuron maturation (Ciceri et al. 2024), suggesting a critical role for other OGID-associated genes in regulating neuronal maturation. Similarly, neuronal maturation was also disrupted in human models of pathogenic *MECP2* mutation modeling Rett Syndrome (Landucci et al. 2018), which disrupts MECP2 read out of DNMT3A-deposited DNA methylation (Clemens et al. 2020; Sandweiss et al. 2020; Pantier et al. 2024). Furthermore, restoring MECP2 expression specifically in GABAergic neurons in Rett mouse models rescued multiple Rett syndrome-associated phenotypes (Ure et al. 2016). Alongside our results, these findings confirm a selective sensitivity of GABAergic neurons to neurodevelopmental disorder (NDD)-associated perturbations that disrupt epigenetic repression of neuronal maturation.

Our HD-MEA results further demonstrate that GABAergic neuron dysfunction is sufficient to imbalance excitatory and inhibitory signaling in TBRS, while such E/I imbalance is a common mechanism suggested to underlie NDD pathogenesis (Gatto and Broadie 2010; Uzunova et al. 2016; Canitano and Pallagrosi 2017; Markicevic et al. 2020; Pietropaolo and Provenzano 2022). Although MEA assessments of NDD models are becoming more prevalent, conclusions from LD-MEA studies are often constrained by a limited quantity of data, often resulting in inconsistent findings both within and across NDD studies (Nageshappa et al. 2016; Marchetto et al. 2017; Amatya et al. 2019; Deneault et al. 2019a; Deneault et al.2 019b; Frega et al. 2019; Alsaqati et al. 2020; Graef et al. 2020; Chapman et al. 2022; DeRosa et al. 2022; Rylaarsdam et al. 2024). Therefore, while LD-MEA assessments in cellular models of Rett Syndrome revealed some phenotypic similarities with our TBRS models (Mok et al. 2022), our study highlights the importance of using HD-MEA to resolve inconsistencies driven by limited data in LD-MEA experiments. Ultimately, the paradigm we present here using HD-MEA provides a high-quality workflow for assessing the role of altered GABAergic neuron function in disrupting neuronal network development, which can be applied across future studies of OGIDs and other NDDs.

In summary, we show that TBRS-associated GABAergic neuron dysfunction is sufficient to disrupt the development of neuronal networks, which is likely to contribute to the etiology of the ASD and ID common among TBRS patients. Furthermore, our findings of molecular and phenotypic relationships between different OGIDs highlight convergent mechanisms likely to underlie their shared clinical presentation. Together, these results suggest that future efforts to develop

interventions for TBRS may have broader applicability across OGIDs, while providing significant information on sensitive cell types and developmental periods that will facilitate the development of such interventions.

Methods

hPSC Model Generation and Culture

Work with hPSCs was performed in accordance with the Washington University Embryonic Stem Cell Research Oversight Committee (ESCRO) under protocol #12-002. DNMT3A R882H iPSCs were reprogrammed from a male patient carrying heterozygous p.R882H (c.2922G>A) mutation and corrected using CRISPR-Cas9 technology. Whole genome sequencing was performed on both the R882H and subsequently corrected control (C-WT) iPSC lines, with summary data in Supplementary Data 1 and full data available from dbGaP (PHS000159). Production of the three primordial germ layers from both R882H and C-WT iPSCs was confirmed by assessing teratoma formation upon iPSC injection into the mouse fat pad.

Del1 and Del2 iPSC models were similarly generated from a male patient with a heterozygous 135 kb deletion containing the entire *DNMT3A* gene. The associated controls (Con1/2) were purchased from FUJIFILM Cellular Dynamics, Inc. (CW20110 and CW20098) as sex matched unrelated controls with no history of neurodevelopmental disorders including autism spectrum disorder and epilepsy. The heterozygous P904L (c.2711C>T) mutation was modelled by its heterozygous introduction into H1 human embryonic stem cells (WT) using CRISPR-Cas9, with the same process generating a model homozygous for small (<10bp) deletions in both alleles of the DNMT3A gene centered on position c.2711 in the cDNA (KO).

DNMT3A CRISPRi lines were created by transducing H1 hESCs with a single vector (Lenti-(BB)-EF1a-KRAB-dCas9-P2A-BlastR) carrying expression cassettes for both dCas9-KRAB and each gRNA. gRNAs (Supplementary Table 1) for DNMT3A from the Dolcetto library (Sanson et al. 2018) were cloned into Lenti-(BB)-EF1a-KRAB-dCas9-P2A-BlastR. Cell lines used to produce induced glutamatergic-like neurons (iGluts) were generated by transducing cell lines with lentivirus carrying pLVX-UbC-rtTA-Ngn2:2A:EGFP. For full details on lentivirus production and stable line generation see Supplementary material.

All hPSC models were maintained under feeder-free conditions on vitronectin in StemFlex Medium and cultured in an incubator with 5% CO2 at 37°C throughout all experiments. Experiments were carried out between passages 20-50 for all hPSC lines and lines periodically tested as negative for mycoplasma contamination.

Modeling cortical GABAergic and glutamatergic neuron development

Modeling of cortical GABAergic neuron development was carried out as previously described (Chapman et al. 2024) by specifying hPSCs as medial ganglionic eminence (MGE)-like progenitors with a ventral telencephalic progenitor (V-NPCs) character and differentiating V-NPCs into immature GABAergic cortical interneurons (V-INs). Cells were collected on day 15 of differentiation as V-NPCs and on day 35 of differentiation as V-INs. Further maturation of V-INs was performed for functional assessments as described below. For full details, see Supplementary Material.

Modeling of cortical glutamatergic neuron development was carried out as previously described (Chapman et al. 2022) with minor modifications by specifying hPSCs as subventricular zone-like progenitors with a dorsal telencephalic progenitor character (D-NPCs) and differentiating these D-NPCs into immature glutamatergic neurons (D-INs). Cells were collected on day 20 of differentiation as D-NPCs and on day 40 of differentiation as D-INs. Further maturation of D-INs was performed for functional assessments as described below. For full details, see Supplementary Material.

Induced glutamatergic-like neurons were generated as previously described (Schafer et al. 2019) by inducing overexpression of Neurogenin-2 (NGN2). Cells were considered iGluts after 14 days of differentiation. For full details see Supplementary Material.

Organoids (Orgs) with a dorsal (D) or ventral (V) telencephalic character were generated by embedding patterned neurospheres, generated during D-NPC or V-NPC specification in Matrigel®. D- and V-Orgs were then maintained on an orbital shaker for a total of 30 days of differentiation; for full details, see Supplementary Material. Organoids were collected and fixed in 4% Paraformaldehyde overnight at 4°C before being incubated in 30% (v/v) sucrose solution overnight at 4°C. Organoids were embedded in a 1:1 ratio of O.C.T compound and 30% sucrose before being sectioned on a cryostat at 8 µm.

Cellular Phenotyping

Changes in DNMT3A expression across TBRS models was assessed by western blot using protein isolated from pluripotent stem cells. Quantifications of neurosphere outgrowth were performed in D-NPCs and V-NPCs after 12 days of differentiation (D12) and changes in proliferation and lineage marker expression were assessed by immunocytochemistry 4 days after D-NPC or V-NPC specification was complete. Analogous quantifications of organoid size, proliferation, and lineage marker expression were made in D-Orgs and V-Orgs after 30 days of differentiation. RT-qPCR to assess changes in the expression of specific genes was also performed from D-NPC and V-NPC samples isolated after specification was complete.

Changes in PIK3/AKT/mTOR signaling were assessed by western blotting using V-NPC samples, and rapamycin (5 nM) was applied to V-NPCs for 4 days after V-NPC specification was complete to assess changes in proliferation upon mTOR inhibition. Similarly, the effects of EZH2 inhibition were assessed by RT-qPCR in D-NPCs treated with EZH2i (GSK343 at 4 µM) versus DMSO or siRNAs targeting EZH2 versus siRNA for GFP for 4 days after specification was complete.

TBRS-associated alterations to neuronal differentiation were assessed by immunocytochemistry for markers of neuronal differentiation in D-Orgs and V-Orgs at D30, with similar quantifications made in V-INs at D40. Neuronal morphology was assessed in V-INs at D30, and synapse production of V-INs was assessed at D50 after V-INs were grown in co-culture with rat astrocytes for 20 days. For further information on the methods described above, see Supplementary Material.

Sequencing

RNA sequencing (RNA-seq) and whole genome bisulfite sequencing (WGBS) was performed as previously described (Hamagami et al. 2023; Chapman et al. 2024) on 882, 904, C-WT, and WT V-NPCs at D15, with similar analysis performed in 882 and C-WT D-NPCs at D20. CUT&Tag for histone H3 lysine 27 tri-methylation was performed as previously described (Chapman et al. 2024) on 882, 904, C-WT and WT V-NPCs at D15. RNA-seq and WGBS were also performed in 882, 904, C-WT and WT D-and V-INs at D40 and D35 respectively with similar analysis performed in 882, 904, C-WT and WT iGluts at D14. For full details on CUT&Tag, RNA-seq and WGBS methodologies see Supplementary Material.

Functional Phenotyping

For electrophysiology, D28 D-INs and D23 V-INs were plated on rat cortical astrocytes and matured until D60, before electrophysiological measurements were generated as described previously (Meganathan et al. 2017). Results were analyzed using non-parametric rank sum tests comparing TBRS models to matched isogenic controls with raw results presented in Supplemental Data.

All low-density multi-electrode array (MEA) experiments were performed using CytoView MEA 48 well plates using co-cultures of matured D-INs and V-INs (at a 70:30 ratio). Electrophysiological activity was recorded every 5 days using hardware (Maestro Edge) and software (AxIS 1.5.2) from Axion Biosystems, with analysis performed using the built-in Axion neural metric analysis tool.

All high-density MEA experiments were performed using CorePlate™ 6W 38/60 MEAs using co-cultures of V-INs and iGluts (at a 30:70 ratio) alongside rat astrocytes. Electrophysiological activity was recorded on D50 and D82 of V-IN differentiation, using the HyperCAM Alpha system (3Brain) and accompanying BrainWave5 software, with primary data analysis performed using BrainWave5 software. For full details on electrophysiological and MEA characterization of TBRS models, see Supplementary Material.

Quantification and Statistical Analysis

Where appropriate, statistical analysis was carried out using GraphPad Prism version 9 (GraphPad Software; La Jolla, CA, USA, available from *www.graphpad.com*) and/or RStudio version 3.5.1 (RStudio: Integrated development environment for R; Boston, MA, USA. Available from *www.rstudio.org*). All technical replicates were averaged before statistical analysis, and statistical tests used for each data analysis are detailed in the figure legends or in detailed methods section for specific analysis paradigms. A minimum of 3 independent differentiations were used for each time point or biological condition, with the number of differentiations used for each sample listed in figure legends as n. The results in figures are presented as group mean +/- standard error (SE), indicating each biological replicate used for the analysis unless otherwise specified in figure legends. Statistical significance is indicated as follows: n.s., not significant; ∗, $p < 0.05$; ∗∗, $p < 0.01$; ∗∗∗, $p < 0.001$; ∗∗∗∗, $p < 0.0001$, unless otherwise specified in figure legends.

Data availability

Raw and processed data was deposited into the Gene Expression Omnibus as accession numbers GSE294191 (DNA methylation), GSE294189 (RNA sequencing) and GSE294186 (H3K27me3 CUT&Tag).

Acknowledgements

This work was supported by NIH Grants R01NS114551, R01MH124808, R01HD110556, and U0-HG007530 (NIH Common Fund/NINDS Undiagnosed Disease Network pilot gene study subaward) to KLK, and by NIH P50HD103525 to Joseph Dougherty and Christina Gurnett (KLK is project PI for the Human Cellular Models Unit of the Washington University Intellectual and Developmental Disabilities Research Center, with project effort funded by this grant). Foundations supporting this work included the Engelhart Family Foundation, Simons Foundation, M-CM Network, and pilot awards from the WU Hope Center, Center of Regenerative Medicine, and Institute for Clinical and Translational Sciences to KLK

We thank the Genome Technology Access Center at the McDonnell Genome Institute at Washington University School of Medicine for help with genomics services. The Center is partially supported by NCI Cancer Center Support Grant #P30 CA91842 to the Siteman Cancer Center from the National Center for Research Resources (NCRR), a component of the National Institutes of Health (NIH) and NIH Roadmap for Medical Research. This publication is solely the responsibility of the authors and does not necessarily represent the official view of NCRR or NIH. We also thank the Genome Engineering & Stem Cell Center (GESC@MGI) at Washington University in St. Louis for cell line engineering services. The DNMT3A R882H iPSC line and Del1/2 iPSC lines used in this study were developed and characterized in the laboratory of Timothy J. Ley at Washington University, by Daniel George and Dr. Christopher A. Miller, supported by NIH CA197161.

Additional information

Author Contributions

G.C. and J.J.D. performed differentiations and MEA assessments and analyzed all results. G.C., J.R.E., and T.E.L. performed computational and bioinformatics analysis. J.E.H and J.J.D. performed electrophysiological assessments and associated analysis. G.C. and S.C. performed qPCR and

associated analysis. G.C., F.B., R.P. and H.J. performed immunocytochemistry assessments, and G.C. and F.B. performed western blotting analysis. H.W.G. and K.L.K. supervised the work. G.C. wrote the manuscript, and all the authors contributed to reviewing and editing the manuscript.

Funding

Funder	Grant reference number	Author
HHS | NIH | National Institute of Neurological Disorders and Stroke (NINDS)	R01NS114551	Kristen L Kroll
HHS | NIH | National Institute of Mental Health (NIMH)	R01MH124808	Kristen L Kroll
HHS | NIH | Eunice Kennedy Shriver National Institute of Child Health and Human Development (NICHD)	R01HD110556	Kristen L Kroll
HHS | NIH | National Institute of Neurological Disorders and Stroke (NINDS)	U0-HG007530	Kristen L Kroll
HHS | NIH | Eunice Kennedy Shriver National Institute of Child Health and Human Development (NICHD)	P50HD103525	Kristen L Kroll

Author ORCID iDs

Gareth Chapman: https://orcid.org/0000-0001-5959-4841
Julianna J Determan: https://orcid.org/0000-0002-4023-9492
Faiza Batool: https://orcid.org/0000-0002-9045-1774
James E Huettner: https://orcid.org/0000-0002-0400-3802
Ramachandran Prakasam: https://orcid.org/0000-0003-0248-7580
Sydney R Crump: https://orcid.org/0009-0008-5341-4238
Travis E Law: https://orcid.org/0000-0002-7399-3299
Haley Jetter: https://orcid.org/0000-0003-0532-2968
Harrison W Gabel: https://orcid.org/0000-0001-6894-5113
Kristen L Kroll: https://orcid.org/0000-0002-5450-6694

Additional files

Supplementary Fig. S1
Supplementary Fig. S2
Supplementary Fig. S3
Supplementary Fig. S4
Supplementary Fig. S5
Supplementary Fig. S6
Supplementary Fig. S7
Supplementary Fig. S8
Supplementary Fig. S9
Supplementary Fig. S10
Supplementary Fig. S11
Supplementary Fig. S12
Supplementary Fig. S13
Supplementary Fig. S14
Supplementary Fig. S15

Supplementary Fig. S16
Supplementary Data 1-2
Supplementary Data 3-4
Supplementary Data 5-6
Supplementary Data 7-10
Supplementary Data 11-13
Supplementary Data 14-15
Supplementary Data 16-20
Supplementary Methods

References

Alsaqati M, Heine VM, Harwood AJ (2020) Pharmacological intervention to restore connectivity deficits of neuronal networks derived from ASD patient iPSC with a TSC2 mutation. *Mol Autism* **11**:80 https://doi.org/10.1186/s13229-020-00391-w | PubMed

Amatya DN, Linker SB, Mendes APD, Santos R, Erikson G, Shokhirev MN, Zhou Y, Sharpee T, Gage FH, Marchetto MC, *et al.* (2019) Dynamical Electrical Complexity Is Reduced during Neuronal Differentiation in Autism Spectrum Disorder. *Stem Cell Reports* **13**:474-484 https://doi.org/10.1016/j.stemcr.2019.08.001 | PubMed

Atterton C, Trew I, Cale JM, Aung-Htut MT, Grens K, Kiernan J, Delagrammatikas CG, Piper M (2025) Overgrowth-intellectual disability disorders: progress in biology, patient advocacy and innovative therapies. *Dis Model Mech* **18** https://doi.org/10.1242/dmm.052300 | PubMed

Bassetti D, Luhmann HJ, Kirischuk S (2021) Effects of Mutations in TSC Genes on Neurodevelopment and Synaptic Transmission. *Int J Mol Sci* **22** https://doi.org/10.3390/ijms22147273 | PubMed

Beard DC, Zhang X, Wu DY, Martin JR, Erickson A, Boua JV, Hamagami N, Swift RG, McCullough KB, Ge X, *et al.* (2023) Distinct disease mutations in DNMT3A result in a spectrum of behavioral, epigenetic, and transcriptional deficits. *Cell Rep* **42**:113411 https://doi.org/10.1016/j.celrep.2023.113411 | PubMed

Canitano R, Pallagrosi M (2017) Autism Spectrum Disorders and Schizophrenia Spectrum Disorders: Excitation/Inhibition Imbalance and Developmental Trajectories. *Front Psychiatry* **8**:69 https://doi.org/10.3389/fpsyt.2017.00069 | PubMed

Chapman G, Alsaqati M, Lunn S, Singh T, Linden SC, Linden DEJ, van den Bree MBM, Ziller M, Owen MJ, Hall J, *et al.* (2022) Using induced pluripotent stem cells to investigate human neuronal phenotypes in 1q21.1 deletion and duplication syndrome. *Mol Psychiatry* **27**:819-830 https://doi.org/10.1038/s41380-021-01182-2 | PubMed

Chapman G, Determan J, Jetter H, Kaushik K, Prakasam R, Kroll KL (2024) Defining cis-regulatory elements and transcription factors that control human cortical interneuron development. *iScience* **27**:109967 https://doi.org/10.1016/j.isci.2024.109967 | PubMed

Chen W, Dai G, Qian Y, Wen L, He X, Liu H, Gao Y, Tang X, Dong B (2022) PIK3CA mutation affects the proliferation of colorectal cancer cells through the PI3K-MEK/PDK1-GPT2 pathway. *Oncol Rep* **47** https://doi.org/10.3892/or.2021.8222 | PubMed

Christian DL, Wu DY, Martin JR, Moore JR, Liu YR, Clemens AW, Nettles SA, Kirkland NM, Papouin T, Hill CA, *et al.* (2020) DNMT3A Haploinsufficiency Results in Behavioral Deficits and Global Epigenomic Dysregulation Shared across Neurodevelopmental Disorders. *Cell Rep* **33**:108416 https://doi.org/10.1016/j.celrep.2020.108416 | PubMed

Ciceri G, Baggiolini A, Cho HS, Kshirsagar M, Benito-Kwiecinski S, Walsh RM, Aromolaran KA, Gonzalez-Hernandez AJ, Munguba H, Koo SY, *et al.* (2024) An epigenetic barrier sets the timing of human neuronal maturation. *Nature* **626**:881-890 https://doi.org/10.1038/s41586-023-06984-8 | PubMed

Clemens AW, Wu DY, Moore JR, Christian DL, Zhao G, Gabel HW (2020) MeCP2 Represses Enhancers through Chromosome Topology-Associated DNA Methylation. *Mol Cell* **77**:279-293. https://doi.org/10.1016/j.molcel.2019.10.033 | PubMed

Cohen AS, Yap DB, Lewis ME, Chijiwa C, Ramos-Arroyo MA, Tkachenko N, Milano V, Fradin M, McKinnon ML, Townsend KN, *et al.* (2016) Weaver Syndrome-Associated EZH2 Protein Variants Show Impaired Histone Methyltransferase Function In Vitro. *Hum Mutat* **37**:301-307 https://doi.org/10.1002/humu.22946 | PubMed

Connacher R, Williams M, Prem S, Yeung PL, Matteson P, Mehta M, Markov A, Peng C, Zhou X, McDermott CR, *et al.* (2022) Autism NPCs from both idiopathic and CNV 16p11.2 deletion patients exhibit dysregulation of proliferation and mitogenic responses. *Stem Cell Reports* **17**:1786 https://doi.org/10.1016/j.stemcr.2022.06.007 | PubMed

Deneault E, Faheem M, White SH, Rodrigues DC, Sun S, Wei W, Piekna A, Thompson T, Howe JL, Chalil L, *et al.* (2019a) CNTN5(-)(/+)or EHMT2(-)(/+)human iPSC-derived neurons from individuals with autism develop hyperactive neuronal networks. *eLife* **8** https://doi.org/10.7554/elife.40092 | PubMed

Deneault E, White SH, Rodrigues DC, Ross PJ, Faheem M, Zaslavsky K, Wang Z, Alexandrova R, Pellecchia G, Wei W, *et al.* (2019b) Complete Disruption of Autism-Susceptibility Genes by Gene Editing Predominantly Reduces Functional Connectivity of Isogenic Human Neurons. *Stem Cell Reports* **12**:427-429 https://doi.org/10.1016/j.stemcr.2019.01.008 | PubMed

DeRosa BA, Hokayem JE, Artimovich E, Garcia-Serje C, Phillips AW, Van Booven D, Nestor JE, Wang L, Cuccaro ML, Vance JM, *et al.* (2022) Author Correction: Convergent Pathways in Idiopathic Autism Revealed by Time Course Transcriptomic Analysis of Patient-Derived Neurons. *Sci Rep* **12**:3445 https://doi.org/10.1038/s41598-022-07356-4 | PubMed

Dobyns WB, Mirzaa GM (2019) Megalencephaly syndromes associated with mutations of core components of the PI3K-AKT-MTOR pathway: PIK3CA, PIK3R2, AKT3, and MTOR. *Am J Med Genet C Semin Med Genet* **181**:582-590 https://doi.org/10.1002/ajmg.c.31736 | PubMed

Ernst C (2016) Proliferation and Differentiation Deficits are a Major Convergence Point for Neurodevelopmental Disorders. *Trends Neurosci* **39**:290-299 https://doi.org/10.1016/j.tins.2016.03.001 | PubMed

Feng J, Chang H, Li E, Fan G (2005) Dynamic expression of de novo DNA methyltransferases Dnmt3a and Dnmt3b in the central nervous system. *J Neurosci Res* **79**:734-746 https://doi.org/10.1002/jnr.20404 | PubMed

Frega M, Linda K, Keller JM, Gumus-Akay G, Mossink B, van Rhijn JR, Negwer M, Klein Gunnewiek T, Foreman K, Kompier N, *et al.* (2019) Neuronal network dysfunction in a model for Kleefstra syndrome mediated by enhanced NMDAR signaling. *Nat Commun* **10**:4928 https://doi.org/10.1038/s41467-019-12947-3 | PubMed

Fu C, Cawthon B, Clinkscales W, Bruce A, Winzenburger P, Ess KC (2012) GABAergic interneuron development and function is modulated by the Tsc1 gene. *Cereb Cortex* **22**:2111-2119 https://doi.org/10.1093/cercor/bhr300 | PubMed

Gatto CL, Broadie K (2010) Genetic controls balancing excitatory and inhibitory synaptogenesis in neurodevelopmental disorder models. *Front Synaptic Neurosci* **2**:4 https://doi.org/10.3389/fnsyn.2010.00004 | PubMed

Gibson WT, Hood RL, Zhan SH, Bulman DE, Fejes AP, Moore R, Mungall AJ, Eydoux P, Babul-Hirji R, An J, *et al.* (2012) Mutations in EZH2 cause Weaver syndrome. *Am J Hum Genet* **90**:110-118 https://doi.org/10.1016/j.ajhg.2011.11.018 | PubMed

Graef JD, Wu H, Ng C, Sun C, Villegas V, Qadir D, Jesseman K, Warren ST, Jaenisch R, Cacace A, *et al.* (2020) Partial FMRP expression is sufficient to normalize neuronal hyperactivity in Fragile X neurons. *Eur J Neurosci* **51**:2143-2157 https://doi.org/10.1111/ejn.14660 | PubMed

Hamagami N, Wu DY, Clemens AW, Nettles SA, Li A, Gabel HW (2023) NSD1 deposits histone H3 lysine 36 dimethylation to pattern non-CG DNA methylation in neurons. *Molecular Cell* **83**:1412-1428. https://doi.org/10.1016/j.molcel.2023.04.001 | PubMed

Kang HJ, Kawasawa YI, Cheng F, Zhu Y, Xu X, Li M, Sousa AM, Pletikos M, Meyer KA, Sedmak G, *et al.* (2011) Spatio-temporal transcriptome of the human brain. *Nature* **478**:483-489 https://doi.org/10.1038/nature10523 | PubMed

Kirmse K, Zhang C (2022) Principles of GABAergic signaling in developing cortical network dynamics. *Cell Rep* **38**:110568 https://doi.org/10.1016/j.celrep.2022.110568 | PubMed

Landucci E, Brindisi M, Bianciardi L, Catania LM, Daga S, Croci S, Frullanti E, Fallerini C, Butini S, Brogi S, *et al.* (2018) iPSC-derived neurons profiling reveals GABAergic circuit disruption and acetylated alpha-tubulin defect which improves after iHDAC6 treatment in Rett syndrome. *Exp Cell Res* **368**:225-235 https://doi.org/10.1016/j.yexcr.2018.05.001 | PubMed

Lane C, Tatton-Brown K, Freeth M (2020) Tatton-Brown-Rahman syndrome: cognitive and behavioural phenotypes. *Dev Med Child Neurol* **62**:993-998 https://doi.org/10.1111/dmcn.14426 | PubMed

Li J, Pinto-Duarte A, Zander M, Cuoco MS, Lai CY, Osteen J, Fang L, Luo C, Lucero JD, Gomez-Castanon R, *et al.* (2022) Dnmt3a knockout in excitatory neurons impairs postnatal synapse maturation and increases the repressive histone modification H3K27me3. *eLife* **11** https://doi.org/10.7554/elife.66909 | PubMed

Makinen ME, Yla-Outinen L, Narkilahti S (2018) GABA and Gap Junctions in the Development of Synchronized Activity in Human Pluripotent Stem Cell-Derived Neural Networks. *Front Cell Neurosci* **12**:56 https://doi.org/10.3389/fncel.2018.00056 | PubMed

Marchetto MC, Belinson H, Tian Y, Freitas BC, Fu C, Vadodaria K, Beltrao-Braga P, Trujillo CA, Mendes APD, Padmanabhan K, *et al.* (2017) Altered proliferation and networks in neural cells derived from idiopathic autistic individuals. *Mol Psychiatry* **22**:820-835 https://doi.org/10.1038/mp.2016.95 | PubMed

Markicevic M, Fulcher BD, Lewis C, Helmchen F, Rudin M, Zerbi V, Wenderoth N (2020) Cortical Excitation:Inhibition Imbalance Causes Abnormal Brain Network Dynamics as Observed in Neurodevelopmental Disorders. *Cereb Cortex* **30**:4922-4937 https://doi.org/10.1093/cercor/bhaa084 | PubMed

Meganathan K, Lewis EMA, Gontarz P, Liu S, Stanley EG, Elefanty AG, Huettner JE, Zhang B, Kroll KL (2017) Regulatory networks specifying cortical interneurons from human embryonic stem cells reveal roles for CHD2 in interneuron development. *Proc Natl Acad Sci U S A* **114**:E11180-E11189 https://doi.org/10.1073/pnas.1712365115 | PubMed

Mirzaa G, Timms AE, Conti V, Boyle EA, Girisha KM, Martin B, Kircher M, Olds C, Juusola J, Collins S, *et al.* (2016) PIK3CA-associated developmental disorders exhibit distinct classes of mutations with variable expression and tissue distribution. *JCI Insight* **1** https://doi.org/10.1172/jci.insight.87623 | PubMed

Mok RSF, Zhang W, Sheikh TI, Pradeepan K, Fernandes IR, DeJong LC, Benigno G, Hildebrandt MR, Mufteev M, Rodrigues DC, *et al.* (2022) Wide spectrum of neuronal and network phenotypes in human stem cell-derived excitatory neurons with Rett syndrome-associated MECP2 mutations. *Transl Psychiatry* **12**:450 https://doi.org/10.1038/s41398-022-02216-1 | PubMed

Nageshappa S, Carromeu C, Trujillo CA, Mesci P, Espuny-Camacho I, Pasciuto E, Vanderhaeghen P, Verfaillie CM, Raitano S, Kumar A, *et al.* (2016) Altered neuronal network and rescue in a human MECP2 duplication model. *Mol Psychiatry* **21**:178-188 https://doi.org/10.1038/mp.2015.128 | PubMed

Nguyen TV, Yao S, Wang Y, Rolfe A, Selvaraj A, Darman R, Ke J, Warmuth M, Smith PG, Larsen NA, *et al.* (2019) The R882H DNMT3A hot spot mutation stabilizes the formation of large DNMT3A oligomers with low DNA methyltransferase activity. *J Biol Chem* **294**:16966-16977 https://doi.org/10.1074/jbc.ra119.010126 | PubMed

Ostrowski PJ, Tatton-Brown K (1993) Tatton-Brown-Rahman Syndrome. In: Adam MP, Feldman J, Mirzaa GM, Pagon RA, Wallace SE, Bean LJH, Gripp KW, Amemiya A (Eds). *GeneReviews((R))* Seattle (WA). PubMed

Pantier R, Brown M, Han S, Paton K, Meek S, Montavon T, Shukeir N, McHugh T, Kelly DA, Hochepied T, *et al.* (2024) MeCP2 binds to methylated DNA independently of phase separation and heterochromatin organisation. *Nat Commun* **15**:3880 https://doi.org/10.1038/s41467-024-47395-1 | PubMed

Pietropaolo S, Provenzano G (2022) Editorial: Targeting Excitation-Inhibition Imbalance in Neurodevelopmental and Autism Spectrum Disorders. *Front Neurosci* **16** https://doi.org/10.3389/fnins.2022.968115 | PubMed

Romanyuk N, Sintakova K, Arzhanov I, Horak M, Gandhi C, Jhanwar-Uniyal M, Jendelova P (2024) mTOR pathway inhibition alters proliferation as well as differentiation of neural stem cells. *Front Cell Neurosci* **18**:1298182 https://doi.org/10.3389/fncel.2024.1298182 | PubMed

Rylaarsdam L, Rakotomamonjy J, Pope E, Guemez-Gamboa A (2024) iPSC-derived models of PACS1 syndrome reveal transcriptional and functional deficits in neuron activity. *Nat Commun* **15**:827 https://doi.org/10.1038/s41467-024-44989-7 | PubMed

Samuels Y, Diaz LA, Schmidt-Kittler O, Cummins JM, Delong L, Cheong I, Rago C, Huso DL, Lengauer C, Kinzler KW, *et al.* (2005) Mutant PIK3CA promotes cell growth and invasion of human cancer cells. *Cancer Cell* **7**:561-573 https://doi.org/10.1016/j.ccr.2005.05.014 | PubMed

Sandweiss AJ, Brandt VL, Zoghbi HY (2020) Advances in understanding of Rett syndrome and MECP2 duplication syndrome: prospects for future therapies. *Lancet Neurol* **19**:689-698 https://doi.org/10.1016/s1474-4422(20)30217-9 | PubMed

Sanson KR, Hanna RE, Hegde M, Donovan KF, Strand C, Sullender ME, Vaimberg EW, Goodale A, Root DE, Piccioni F, *et al.* (2018) Optimized libraries for CRISPR-Cas9 genetic screens with multiple modalities. *Nat Commun* **9**:5416 https://doi.org/10.1038/s41467-018-07901-8 | PubMed

Schafer ST, Paquola ACM, Stern S, Gosselin D, Ku M, Pena M, Kuret TJM, Liyanage M, Mansour AA, Jaeger BN, *et al.* (2019) Pathological priming causes developmental gene network heterochronicity in autistic subject-derived neurons. *Nat Neurosci* **22**:243-255 https://doi.org/10.1038/s41593-018-0295-x | PubMed

Smith AM, LaValle TA, Shinawi M, Ramakrishnan SM, Abel HJ, Hill CA, Kirkland NM, Rettig MP, Helton NM, Heath SE, *et al.* (2021) Functional and epigenetic phenotypes of humans and mice with DNMT3A Overgrowth Syndrome. *Nat Commun* **12**:4549 https://doi.org/10.1038/s41467-021-24800-7 | PubMed

Tatton-Brown K, Loveday C, Yost S, Clarke M, Ramsay E, Zachariou A, Elliott A, Wylie H, Ardissone A, Rittinger O, *et al.* (2017) Mutations in Epigenetic Regulation Genes Are a Major Cause of Overgrowth with Intellectual Disability. *Am J Hum Genet* **100**:725-736 https://doi.org/10.1016/j.ajhg.2017.03.010 | PubMed

Tatton-Brown K, Murray A, Hanks S, Douglas J, Armstrong R, Banka S, Bird LM, Clericuzio CL, Cormier-Daire V, Cushing T, *et al.* (2013) Weaver syndrome and EZH2 mutations: Clarifying the clinical phenotype. *Am J Med Genet A* **161A**:2972-2980 https://doi.org/10.1002/ajmg.a.36229 | PubMed

Tatton-Brown K, Zachariou A, Loveday C, Renwick A, Mahamdallie S, Aksglaede L, Baralle D, Barge-Schaapveld D, Blyth M, Bouma M, *et al.* (2018) The Tatton-Brown-Rahman Syndrome: A clinical study of 55 individuals with de novo constitutive DNMT3A variants. *Wellcome Open Res* **3**:46 https://doi.org/10.12688/wellcomeopenres.14430.1 | PubMed

Thomas H, Alix T, Renard E, Renaud M, Wourms J, Zuily S, Leheup B, Genevieve D, Dreumont N, Schmitt E, *et al.* (2024) Expanding the genetic and clinical spectrum of Tatton-Brown-Rahman syndrome in a series of 24 French patients. *J Med Genet* https://doi.org/10.1136/jmg-2024-110031 | PubMed

Ure K, Lu H, Wang W, Ito-Ishida A, Wu Z, He LJ, Sztainberg Y, Chen W, Tang J, Zoghbi HY (2016) Restoration of Mecp2 expression in GABAergic neurons is sufficient to rescue multiple disease features in a mouse model of Rett syndrome. *eLife* **5** https://doi.org/10.7554/elife.14198 | PubMed

Uzunova G, Pallanti S, Hollander E (2016) Excitatory/inhibitory imbalance in autism spectrum disorders: Implications for interventions and therapeutics. *World J Biol Psychiatry* **17**:174-186 https://doi.org/10.3109/15622975.2015.1085597 | PubMed

Wang L, Huang D, Jiang Z, Luo Y, Norris C, Zhang M, Tian X, Tang Y (2017) Akt3 is responsible for the survival and proliferation of embryonic stem cells. *Biol Open* **6**:850-861 https://doi.org/10.1242/bio.024505 | PubMed

Wang M, Wei PC, Lim CK, Gallina IS, Marshall S, Marchetto MC, Alt FW, Gage FH (2020) Increased Neural Progenitor Proliferation in a hiPSC Model of Autism Induces Replication Stress-Associated Genome Instability. *Cell Stem Cell* **26**:221-233. https://doi.org/10.1016/j.stem.2019.12.013 | PubMed

Watanabe D, Uchiyama K, Hanaoka K (2006) Transition of mouse de novo methyltransferases expression from Dnmt3b to Dnmt3a during neural progenitor cell development. *Neuroscience* **142**:727-737 https://doi.org/10.1016/j.neuroscience.2006.07.053 | PubMed

Wu Z, Huang K, Yu J, Le T, Namihira M, Liu Y, Zhang J, Xue Z, Cheng L, Fan G (2012) Dnmt3a regulates both proliferation and differentiation of mouse neural stem cells. *J Neurosci Res* **90**:1883-1891 https://doi.org/10.1002/jnr.23077 | PubMed

Ziller MJ, Ortega JA, Quinlan KA, Santos DP, Gu H, Martin EJ, Galonska C, Pop R, Maidl S, Di Pardo A, *et al.* (2018) Dissecting the Functional Consequences of De Novo DNA Methylation Dynamics in Human Motor Neuron Differentiation and Physiology. *Cell Stem Cell* **22**:559-574. https://doi.org/10.1016/j.stem.2018.02.012 | PubMed

Peer reviews

Reviewer #1 (Public review):

Summary:

This is an important study that describes the consequences of the DNMT3A mutation in human neuronal development for the first time. The selective impact of DNMT3A function on GABAergic interneurons is interesting and an important feature of future therapeutics. The claims made in that manuscript are supported by strong evidence for the most part. And the data are of high quality in general and presented well.

Strengths:

The strengths of the work include: Characterization of multiple DNMT3A loss-of-function alleles, including two misense variants, R882H, P904L, and a deletion allele. The missense mutation lines both include an ideal control with the same genetic background. The CRISPRi-mediated DNMT3A knockdown has also been included. The study identifies the mTOR-PI3K pathway as a factor of overgrowth issues found in the mutant organoid. In bulk mRNA sequencing and whole-genome bisulfite sequencing, identify hypomethylated genomic regions associated with gene expression repression. Again, this is more pronounced in the ventral organoid compared to the dorsal organoid. In addition, the extensive electrophysiological characterizations with a high-density microelectrode array support the more mature status of mutant interneurons.

Weaknesses:

Although a strong study overall, some weaknesses are noted. These include:

(1) The lack of validation data for the generated iPSCs and hESCs, such as the chromosomal contents, ploidy, and pluripotency states.

(2) Other weaknesses relate to data interpretation and insufficient discussion of related matters, as detailed in the recommendations to the authors.

(3) Also, some errors are noted and detailed in the recommendation section.

https://doi.org/10.7554/eLife.111056.1.sa3

Reviewer #2 (Public review):

Summary:

Chapman, Determan et al. investigate how pathogenic mutations in DNMT3A, which cause Tatton-Brown-Rahman Syndrome (TBRS), disrupt human cortical developmental processes using a comprehensive panel of human pluripotent stem cell models spanning DNMT3A loss-of-function severity. The authors aim to identify the cellular and molecular mechanisms underlying TBRS-associated brain overgrowth and intellectual disability, and to test whether mechanistic convergence exists between TBRS and other overgrowth-intellectual disability disorders (OGIDs) caused by mutations in EZH2 (Weaver syndrome) or PIK3CA pathway components. Their central conclusion is that GABAergic interneuron development is selectively vulnerable to DNMT3A mutation, where reduced DNA methylation causes premature de-repression of neuronal and synaptic genes, driving precocious neuronal maturation and hyperactivity sufficient to disrupt neuronal network synchrony. This report adds to a growing literature supporting the vulnerability of GABAergic interneurons in NDDs and further provides a mechanistic view of this vulnerability, potentially convergent across OGIDs. The mechanistic claims around H3K27me3 compensation and mTOR-based therapeutic convergence, while promising, rest on more preliminary evidence and would benefit from the distinction between correlation and mechanism being made more explicit in the text. Overall, this is a compelling study with a rigorous experimental design and novel findings with a potential impact on a better understanding of the OGID pathophysiology.

Strengths:

(1) A major strength of this work is the breadth and rigor of the disease modeling approach. Four independent TBRS model systems are used in tandem: a patient-derived iPSC line with isogenic CRISPR-corrected control (R882H), a knock-in hESC model (P904L) with its wild-type isogenic, patient deletion iPSC lines (Del1/2), and CRISPRi knockdown models (G1/G2), collectively spanning a range of DNMT3A loss-of-function that correlates with phenotypic severity. This allelic series design substantially strengthens causal inference beyond what any single isogenic pair could provide.

(2) The multi-omic integration across matched developmental stages provides a strong mechanistic foundation for the cellular phenotyping and provides significantly enhanced novelty. RNA-seq, whole-genome bisulfite sequencing, and H3K27me3 CUT&Tag are combined in the same cell types, and timepoints show that DNMT3A loss reduces CG methylation at neuronal and synaptic gene loci, leading to premature transcriptional activation.

(3) The selective vulnerability of ventral (GABAergic) versus dorsal (glutamatergic) progenitors is one of the study's most important findings. This lineage specificity is consistently observed across all model systems and in both 2D and organoid formats, where ventral NPCs show increased proliferation, premature neuronal gene expression, and increased neurogenesis, while dorsal NPCs are largely unaffected at the transcriptomic and cellular level despite exhibiting comparable DNA methylation changes. This adds to a body of emerging work showing GABAergic interneuron vulnerability in NDDs where ubiquitously expressed genes such as chromatin modifiers are perturbed, and provides additional molecular insights into potential mechanisms of "resilience" of dorsal populations.

(4) The functional characterization follows a logical progression from single-neuron electrophysiology (demonstrating GABAergic hyperactivity with increased action potential amplitude and firing rate) to network-level analysis using high-density multi-electrode arrays. The HD-MEA experimental design - pairing TBRS or control GABAergic neurons with a constant background of control iGlut neurons - cleanly isolates GABAergic dysfunction as the driver of network hypersynchrony.

Weaknesses:

(1) The concomitant induction of proliferation and differentiation in TBRS V-NPCs is conceptually striking, since these are generally considered antagonistic developmental programs. The authors partially address this tension by noting that DNMT3A LOF alone is insufficient to initiate neuronal differentiation, i.e., V-NPCs upregulate neuronal and synaptic genes while retaining progenitor identity, implying that transcriptomic priming and commitment to differentiation are decoupled. However, the relationship between the proliferative phenotype and the epigenetic priming phenotype remains mechanistically unresolved. The manuscript documents mTOR pathway upregulation at the protein level and identifies shared DEGs that include proliferative regulators, but it does not establish whether mTOR-driven proliferation and mCG-loss-driven neuronal gene de-repression/enhanced differentiation are causally linked or represent two independent consequences of DNMT3A LOF.

(2) Relatedly, the rapamycin rescue experiment is a valuable proof-of-concept for the PIK3/AKT/mTOR convergence but is limited to a single dose in a single model (882) with a single readout (Ki67+ proliferation). Given the prominence of mTOR pathway convergence in the manuscript as a potential shared therapeutic avenue across OGIDs, the data supporting this claim are somewhat preliminary. It remains unknown whether mTOR inhibition rescues downstream phenotypes (neurogenesis, gene expression, neuronal maturation) or whether less severe TBRS models respond similarly. This might also help tackle the first comment above. e.g., if mTOR inhibition rescued proliferation but not the transcriptomic priming, that would support two independent mechanisms.

(3) The claim that H3K27me3 compensates for mCG loss is an important mechanistic point, but the current data do not distinguish between active compensation, in which EZH2 is recruited in response to methylation loss, and functional redundancy, in which H3K27me3 is independently established and becomes the dominant repressive mark once DNA methylation is reduced. The EZH2 knockdown/inhibition experiments show that H3K27me3 is sufficient to maintain repression at hypo-DMR sites, but they do not establish that H3K27me3 gain is itself a response to methylation loss. Because H3K27me3 profiling was performed only in the severe 882 model, it is also unclear whether H3K27me3 gain scales with DNMT3A LOF severity, as a compensatory model would predict. Finally, the EZH2 overexpression rescue is performed in V-NPCs, whereas the compensation model is developed primarily in D-NPCs, making it difficult to assess whether the same mechanism operates in the lineage where it was originally inferred.

(4) The narrative framing of dorsal neuron development as unaffected by DNMT3A LOF is somewhat at odds with the data presented. The 882 D-NPCs show substantial DNA methylation changes, and TBRS D-INs exhibit what the authors describe as "substantive transcriptomic differences" involving persistent expression of pluripotency and progenitor genes, which seems to be a distinct but potentially significant phenotype. The impact of DNMT3A loss between ventral and dorsal lineages might be more accurately framed as divergent in nature rather than specific to a certain population.

(5) SST stainings are not entirely convincing. They appear mostly nuclear, and some instances localized to rosettes in organoids, whereas the protein is largely confined to processes and is expected to be found outside progenitor-rich zones like rosettes.

https://doi.org/10.7554/eLife.111056.1.sa2

Reviewer #3 (Public review):

Summary:

In this manuscript, the authors investigated TBRS etiology by using new human pluripotent stem cell models, modeling varying levels of TBRS-associated loss of DNMT3A function. They identified increased lineage-specific proliferation of precursors in TBRS ventral MGE-like progenitors, which they propose was related to increased signaling through the PIK3/AKT/mTOR pathway. Furthermore, they show that reduced DNA methylation during MGE-like progenitor differentiation into GABAergic interneurons can cause a premature expression of neuronal and synaptic genes, triggering precocious neuronal maturation. In conclusion, they propose that TBRS-derived GABAergic neurons exhibit hyperactivity that can alters the development and structure of neuronal networks.

Strengths:

Overall, the data presented is convincing, from an early developmental point of view, given that the iPSC-derived 2D cultures or organoids used do not get to reach a mature state. Nonetheless, the data clearly show the effects that deleterious mutations in TBRS can cause during the period of neurogenesis, which was missing in the field.

Weaknesses:

(1) Li et al., 2022 (referred to in the manuscript) seems to already show the interplay between H3K27me3 and Dnmt3a discussed in this study i.e., that in the absence of DNA methylation, there is an expansion of polycomb-like repression. These data should be better acknowledged in the paragraph 'Repressive H3K27me3 compensates for severe loss of DNA methylation' (page 9), given it supports the data presented in this manuscript and suggests this as a common mechanism in the interplay between these two repressive marks, as it is well established in the literature.

(2) The authors should acknowledge that the omics data come from a mixed population of cells.

(3) The authors are encouraged to further discuss whether the overgrowth observed in ventral GABAergic cultures or organoids compares to the overgrowth observed in diseased patients. One expects MRIs to have been performed in patients and that these could be harnessed to discern if overgrowth occurs in the cortex or ventral regions of the brain.

https://doi.org/10.7554/eLife.111056.1.sa1

Author response:

> ***Public Reviews:***
>
> ***Reviewer #1 (Public review):***
>
> *Summary:*
>
> *This is an important study that describes the consequences of the DNMT3A mutation in human neuronal development for the first time. The selective impact of DNMT3A function on GABAergic interneurons is interesting and an important feature of future therapeutics. The claims made in that manuscript are supported by strong evidence for the most part. And the data are of high quality in general and presented well.*
>
> *Strengths:*
>
> *The strengths of the work include: Characterization of multiple DNMT3A loss-of-function alleles, including two misense variants, R882H, P904L, and a deletion allele. The missense mutation lines both include an ideal control with the same genetic background. The CRISPRi-mediated DNMT3A knockdown has also been included. The study identifies the mTOR-PI3K pathway as a factor of overgrowth issues found in the mutant organoid. In*

> *bulk mRNA sequencing and whole-genome bisulfite sequencing, identify hypomethylated genomic regions associated with gene expression repression. Again, this is more pronounced in the ventral organoid compared to the dorsal organoid. In addition, the extensive electrophysiological characterizations with a high-density microelectrode array support the more mature status of mutant interneurons.*
>
> *Weaknesses:*
>
> *Although a strong study overall, some weaknesses are noted. These include:*
>
> *(1) The lack of validation data for the generated iPSCs and hESCs, such as the chromosomal contents, ploidy, and pluripotency states.*

We thank the reviewer for their constructive feedback. We previously validated our 882 models with whole genome sequencing and teratoma formation upon mouse fat pad injection, while the parental human embryonic stem cell line (WA01 hESCs) used for P904L variant knock-in was validated by our Genome Engineering Stem Cell (GESC) core upon derivation of that variant knock-in model. We have now added both karyotyping and pluripotency staining (SOX2/OCT4) for all other hPSC lines as (new) Supplementary Figure S17 and included further description in our Methods section under "hPSC Model Generation and Culture".

New Data: Supplemental Figure S17 (SOX2/OCT4 staining in hPSCs and karyotyping of all lines used)

Text edits: Additional language confirming hPSC line validation will be added to the Methods section under "hPSC Model Generation and Culture" on page 18.

> *(2) Other weaknesses relate to data interpretation and insufficient discussion of related matters, as detailed in the recommendations to the authors.*

We thank the reviewer for their insightful suggestions and have detailed our responses in the "recommendations to the authors" section.

> *(3) Also, some errors are noted and detailed in the recommendation section.*

We thank the reviewer for catching these errors and have since corrected them, with detailed responses below.

> ***Reviewer #2 (Public review):***
>
> *Summary:*
>
> *Chapman, Determan et al. investigate how pathogenic mutations in DNMT3A, which cause Tatton-Brown-Rahman Syndrome (TBRS), disrupt human cortical developmental processes using a comprehensive panel of human pluripotent stem cell models spanning DNMT3A loss-of-function severity. The authors aim to identify the cellular and molecular mechanisms underlying TBRS-associated brain overgrowth and intellectual disability, and to test whether mechanistic convergence exists between TBRS and other overgrowth-intellectual disability disorders (OGIDs) caused by mutations in EZH2 (Weaver syndrome) or PIK3CA pathway components. Their central conclusion is that GABAergic interneuron development is selectively vulnerable to DNMT3A mutation, where reduced DNA methylation causes premature de-repression of neuronal and synaptic genes, driving precocious neuronal maturation and hyperactivity sufficient to disrupt neuronal network synchrony. This report adds to a growing literature supporting the vulnerability of GABAergic interneurons in NDDs and further provides a mechanistic view of this vulnerability, potentially convergent across OGIDs. The mechanistic claims around H3K27me3 compensation and mTOR-based therapeutic convergence, while promising,*

rest on more preliminary evidence and would benefit from the distinction between correlation and mechanism being made more explicit in the text. Overall, this is a compelling study with a rigorous experimental design and novel findings with a potential impact on a better understanding of the OGID pathophysiology.

Strengths:

(1) A major strength of this work is the breadth and rigor of the disease modeling approach. Four independent TBRS model systems are used in tandem: a patient-derived iPSC line with isogenic CRISPR-corrected control (R882H), a knock-in hESC model (P904L) with its wild-type isogenic, patient deletion iPSC lines (Del1/2), and CRISPRi knockdown models (G1/G2), collectively spanning a range of DNMT3A loss-of-function that correlates with phenotypic severity. This allelic series design substantially strengthens causal inference beyond what any single isogenic pair could provide.

(2) The multi-omic integration across matched developmental stages provides a strong mechanistic foundation for the cellular phenotyping and provides significantly enhanced novelty. RNA-seq, whole-genome bisulfite sequencing, and H3K27me3 CUT&Tag are combined in the same cell types, and timepoints show that DNMT3A loss reduces CG methylation at neuronal and synaptic gene loci, leading to premature transcriptional activation.

(3) The selective vulnerability of ventral (GABAergic) versus dorsal (glutamatergic) progenitors is one of the study's most important findings. This lineage specificity is consistently observed across all model systems and in both 2D and organoid formats, where ventral NPCs show increased proliferation, premature neuronal gene expression, and increased neurogenesis, while dorsal NPCs are largely unaffected at the transcriptomic and cellular level despite exhibiting comparable DNA methylation changes. This adds to a body of emerging work showing GABAergic interneuron vulnerability in NDDs where ubiquitously expressed genes such as chromatin modifiers are perturbed, and provides additional molecular insights into potential mechanisms of "resilience" of dorsal populations.

(4) The functional characterization follows a logical progression from single-neuron electrophysiology (demonstrating GABAergic hyperactivity with increased action potential amplitude and firing rate) to network-level analysis using high-density multi-electrode arrays. The HD-MEA experimental design - pairing TBRS or control GABAergic neurons with a constant background of control iGlut neurons - cleanly isolates GABAergic dysfunction as the driver of network hypersynchrony.

Weaknesses:

(1) The concomitant induction of proliferation and differentiation in TBRS V-NPCs is conceptually striking, since these are generally considered antagonistic developmental programs. The authors partially address this tension by noting that DNMT3A LOF alone is insufficient to initiate neuronal differentiation, i.e., V-NPCs upregulate neuronal and synaptic genes while retaining progenitor identity, implying that transcriptomic priming and commitment to differentiation are decoupled. However, the relationship between the proliferative phenotype and the epigenetic priming phenotype remains mechanistically unresolved. The manuscript documents mTOR pathway upregulation at the protein level and identifies shared DEGs that include proliferative regulators, but it does not establish whether mTOR-driven proliferation and mCG-loss-driven neuronal gene de-repression/enhanced differentiation are causally linked or represent two independent consequences of DNMT3A LOF.

We thank the reviewer for their comment and agree that this phenotype, whereby progenitors exhibited both increased proliferation and hallmarks of gene expression

associated with neuronal differentiation is striking and interesting, given that these are typically antagonistic paradigms during normal development.

We documented that these phenotypes involve upregulated expression of both neuronal/synaptic and proliferative genes in V-NPCs (Figure 2d), with concomitant loss of repressive DNA methylation at regulatory elements associated with these genes (Figure 2f, Supplemental Data 5). In this work, *DNMT3A* mutation had a more prominent role in de-repressing neuronal and synaptic gene expression to promote hallmarks of neuron differentiation, while playing a relatively less central role in direct regulation of proliferation genes, as seen from the relative prominence of neuronal/synaptic- versus proliferation-related GO terms in our Supplemental Data 5 table.

To examine the mechanisms underlying increased V-NPC proliferation in our TBRS models, we assessed a potential relationship with the PIK3/AKT/mTOR pathway, as this is implicated in increased proliferation resulting from *DNMT3A*-associated mutation in myeloid leukemia (Dai et al., 2017, PMID: 28461508). In our work, *DNMT3A* mutation increased the expression and/or phosphorylation of mTOR signaling pathway targets specifically in V-NPCs (Figure 1q-r, Supplemental Figure S3a-d). However, while TBRS mutation directly affected repressive DNA methylation at a suite of cell proliferation-related genes, these did not include the PIK3/AKT/mTOR pathway genes themselves, suggesting an indirect relationship between altered DNA methylation and increased mTOR signaling.

Text Edits: We will incorporate further discussion of how DNMT3A-mediated gene repression and levels of PIK3/AKT/mTOR pathway signaling may be interacting, providing a framework for future studies to identify how these related OGID gene mutations may converge mechanistically.

> *(2) Relatedly, the rapamycin rescue experiment is a valuable proof-of-concept for the PIK3/AKT/mTOR convergence but is limited to a single dose in a single model (882) with a single readout (Ki67+ proliferation). Given the prominence of mTOR pathway convergence in the manuscript as a potential shared therapeutic avenue across OGIDs, the data supporting this claim are somewhat preliminary. It remains unknown whether mTOR inhibition rescues downstream phenotypes (neurogenesis, gene expression, neuronal maturation) or whether less severe TBRS models respond similarly. This might also help tackle the first comment above. e.g., if mTOR inhibition rescued proliferation but not the transcriptomic priming, that would support two independent mechanisms.*

We thank the reviewer for their comment. We explored both the overall levels and phosphorylation of proteins involved in PIK3/AKT/mTOR signaling in the 882, 904, Del1, Del2, and KO V-NPC models (Figure 1q-r, Supplementary Figure S3a-d), finding specific increases of all proteins. We showed that rapamycin addition reversed the increased proportion of KI67+ proliferating cell nuclei resulting from 882 mutation in V-NPCs in main Figure 1s, while demonstrating that rapamycin also reduced the proportion of KI67+ nuclei observed in both less severe 904 and Del1 V-NPC models (Supplementary Figure S3e-f).

We agree that understanding whether rapamycin treatment can rescue TBRS neuronal phenotypes would be very interesting, as previous work on Tuberous Sclerosis Complex has utilized rapamycin and other mTOR inhibitors to effectively reverse TSC-related alterations of neuronal morphology and neuronal hyperexcitability (Buttermore et al., 2025, PMID: 40792287). Future studies examining convergent mechanisms and therapeutics for OGIDs should examine how similarly targeting this and related pathways rescues altered neuronal morphology, maturation, and function, as we have demonstrated that TBRS mutation has subsequent consequences for V-IN differentiation, maturation, and function. This point has been detailed in the discussion section on pages 15-16.

> *(3) The claim that H3K27me3 compensates for mCG loss is an important mechanistic point, but the current data do not distinguish between active compensation, in which EZH2 is recruited in response to methylation loss, and functional redundancy, in which H3K27me3 is independently established and becomes the dominant repressive mark*

> *once DNA methylation is reduced. The EZH2 knockdown/inhibition experiments show that H3K27me3 is sufficient to maintain repression at hypo-DMR sites, but they do not establish that H3K27me3 gain is itself a response to methylation loss. Because H3K27me3 profiling was performed only in the severe 882 model, it is also unclear whether H3K27me3 gain scales with DNMT3A LOF severity, as a compensatory model would predict. Finally, the EZH2 overexpression rescue is performed in V-NPCs, whereas the compensation model is developed primarily in D-NPCs, making it difficult to assess whether the same mechanism operates in the lineage where it was originally inferred.*

We thank the reviewer for the opportunity to clarify our findings and experimental reasoning. A previous study using a conditional *Dnmt3a* knockout mouse model (Li et al., 2022, PMID: 35604009) demonstrated increased expression of multiple PRC2 components following the loss of Dnmt3a. This study demonstrated that sites which lost DNA methylation gained H3K27me3 in postnatal neurons upon Dnmt3a loss. Therefore, we hypothesize that the gain of H3K27me3 likely occurs in response to loss of DNMT3A methylation.

While we did not perform CUT&Tag for H3K27me3 in our less severe models, we did validate gene expression changes following EZH2 knockdown and inhibition in both the R882H (Figure 4g-h) and P904L (Supplementary Figure S8b) models, finding that gene expression was unchanged in the model with the less severe DNMT3A mutation (P904L). Based upon these findings, we hypothesized that compensatory H3K27me3 may occur only upon severe DNMT3A loss, as seen in the dominant-negative R882H model. Furthermore, as H3K27me3 compensation was more prominent in D-NPCs, we hypothesized that this might be sufficient to prevent de-repression and aberrant neuronal gene repression upon loss of DNMT3A-mediated repression in D-NPCs. However, since TBRS mutation caused the most prominent de-repression of neuronal gene expression in V-NPCs, we also tested whether EZH2 overexpression could reverse this, finding that it partially suppressed this dysregulated neuronal gene expression. To better clarify this logic and the findings, we will make text edits to this results section.

Text edits: We will clarify the reasoning for performing the EZH2 overexpression experiments in V-NPCs and reference Li et al., 2022 in both the results (pg. 9-10) and discussion.

> *(4) The narrative framing of dorsal neuron development as unaffected by DNMT3A LOF is somewhat at odds with the data presented. The 882 D-NPCs show substantial DNA methylation changes, and TBRS D-INs exhibit what the authors describe as "substantive transcriptomic differences" involving persistent expression of pluripotency and progenitor genes, which seems to be a distinct but potentially significant phenotype. The impact of DNMT3A loss between ventral and dorsal lineages might be more accurately framed as divergent in nature rather than specific to a certain population.*

We thank the reviewer for their comment. While TBRS mutations appear to have a significantly stronger effect on V-NPCs and subsequently V-INs, both transcriptomic and methylation alterations do also occur upon TBRS mutation in D-NPCs and D-INs, as noted in Supplemental Figure S4d, S11, and Supplemental Data 2. However, we observed substantially greater molecular alterations in V-NPCs/V-INs, a lack of overt cellular phenotypes in D-NPCs where assayed, and a lack of functional consequences in matured D-INs, suggesting a more significant requirement for DNMT3A in regulating the differentiation and subsequent maturation of cortical inhibitory interneurons during embryonic and early pre-natal development, the developmental periods that we can readily model in hPSC-derived neurons.

It should also be noted that these hPSC differentiation models do not recapitulate post-natal deposition of non-CpG (mCA) DNA methylation, a mechanism disrupted postnatally by TBRS-associated mutations in our prior work in murine models (Harrison Gabel; e.g. Beard et al., 2023, PMID: 37952155). Therefore, we hypothesize that if we could sufficiently mature D-INs to a state that modeled postnatal development and recapitulated this non-CpG methylation, we might be able to detect cellular and functional phenotypes in later stage D-INs. To avoid

misinterpretation, we will alter the language in the results section to confirm that there are both transcriptomic and methylation changes in our D-NPCs/D-INs, but that these are not accompanied by cellular phenotypes or neuronal dysfunction.

Text edits: We will better clarify that there are transcriptomic and methylation changes in D-NPCs/D-INs, but that these changes are minimal compared to those in V-NPCs/V-INs, as supported by the lack of cellular and functional phenotypes seen in D-NPCs/D-INs.

> *(5) SST stainings are not entirely convincing. They appear mostly nuclear, and some instances localized to rosettes in organoids, whereas the protein is largely confined to processes and is expected to be found outside progenitor-rich zones like rosettes.*

We agree that the perinuclear SST staining detected in these young ventral telencephalic-patterned organoids at day 30 differs somewhat from the more process-localized and cytosolic signal seen in later stage organoids in other studies. This may be related to the use of different commercial SST antibodies across studies but also likely reflects SST immunoreactivity in newborn neurons near the onset of SST expression. For example, immature SST-immunoreactive neurons in the early postnatal rat cortex exhibit predominant SST staining in perinuclear cytoplasm and short processes (e.g. Fig. 3 in Lee et al, PMID: 9664223) while acquiring more cytosolic and process-localized staining as postnatal neuron maturation occurs. Evaluation of immunopositivity for other markers of neurogenesis (ASCL1) and immature neurons (TUJ1) is also congruent with these findings for SST, with TBRS-associated mutations increasing in the fraction of cells in V-NPCs/V-ORGs that express these three markers.

> ***Reviewer #3 (Public review):***
>
> *Summary:*
>
> *In this manuscript, the authors investigated TBRS etiology by using new human pluripotent stem cell models, modeling varying levels of TBRS-associated loss of DNMT3A function. They identified increased lineage-specific proliferation of precursors in TBRS ventral MGE-like progenitors, which they propose was related to increased signaling through the PIK3/AKT/mTOR pathway. Furthermore, they show that reduced DNA methylation during MGE-like progenitor differentiation into GABAergic interneurons can cause a premature expression of neuronal and synaptic genes, triggering precocious neuronal maturation. In conclusion, they propose that TBRS-derived GABAergic neurons exhibit hyperactivity that can alters the development and structure of neuronal networks.*
>
> *Strengths:*
>
> *Overall, the data presented is convincing, from an early developmental point of view, given that the iPSC-derived 2D cultures or organoids used do not get to reach a mature state. Nonetheless, the data clearly show the effects that deleterious mutations in TBRS can cause during the period of neurogenesis, which was missing in the field.*
>
> *Weaknesses:*
>
> *(1) Li et al., 2022 (referred to in the manuscript) seems to already show the interplay between H3K27me3 and Dnmt3a discussed in this study i.e., that in the absence of DNA methylation, there is an expansion of polycomb-like repression. These data should be better acknowledged in the paragraph 'Repressive H3K27me3 compensates for severe loss of DNA methylation' (page 9), given it supports the data presented in this manuscript and suggests this as a common mechanism in the interplay between these two repressive marks, as it is well established in the literature.*

We thank the reviewer for this suggestion and will incorporate this reference into both the results and the discussion when discussing the respective roles of DNMT3A and PCR2-mediated repression.

Text edits: We will add Li et al., 2022 to both the results section (pg. 9-10) and our discussion section.

> *(2) The authors should acknowledge that the omics data come from a mixed population of cells.*

We thank the reviewer for their comment. We have validated that the established 2-D differentiation methods we used in this study generate cell populations with >85-90% enrichment for the desired progenitor and neuronal cell type, based upon marker expression, but acknowledge that these are bulk -omics data obtained from cells that may represent a mixed population and have now detailed this in the methods section under “Sequencing”.

Text edits: we will add language acknowledging that our omics data (bulk) was generated from mixed populations of cells.

> *(3) The authors are encouraged to further discuss whether the overgrowth observed in ventral GABAergic cultures or organoids compares to the overgrowth observed in diseased patients. One expects MRIs to have been performed in patients and that these could be harnessed to discern if overgrowth occurs in the cortex or ventral regions of the brain.*

We thank the reviewer for their suggestion and do note that at least one published study documents increased cortical thickness in the MRIs of TBRS patients (Jiménez de la Peña et al., 2024, PMID: 37795572); however, to our knowledge studies have not examined regional or cell type-selective overgrowth of cortical tissue in TBRS patients. Future clinical studies examining the nature of the neuronal progenitor overgrowth and resulting consequences for patient brain imaging would be of interest to better understand TBRS-associated etiology of brain overgrowth and its manifestations.

https://doi.org/10.7554/eLife.111056.1.sa0